12-2021

An Investigation of the Flexural Strength and Toughness of Hybrid Plain and Fiber Reinforced Concrete for Pavement Applications

Wesley Keys
University of Arkansas, Fayetteville

An Investigation of the Flexural Strength and Toughness of Hybrid Plain and Fiber Reinforced Concrete for Pavement Applications

A thesis submitted in partial fulfillment
of the requirements for the degree of
Master of Science in Civil Engineering

by

Wesley Keys
University of Arkansas
Bachelor of Science in Civil Engineering, 2020

December 2021
University of Arkansas

This thesis is approved for recommendation to the Graduate Council.

_____
Cameron Murray, Ph.D.
Thesis Director

_____
Micah Hale, Ph.D.
Committee Member

_____
Ernie Heymsfield, Ph.D.
Committee Member

Abstract

For decades, many solutions have been evaluated to combat cracking in concrete pavements. The study presented in this paper evaluates and compares the flexural performance under a third point loading configuration of plain concrete (PC) beams, fully fiber reinforced concrete (FRC) beams, and hybrid PC and FRC beams, with a top PC and bottom FRC layer. The purpose of this hybrid approach was to provide FRC in only half the section, saving cost, while providing a PC surface layer that is easier to finish. All PC top layers were applied at an age of 7-days, considered a reasonable time for constructability of a pavement. Four different types of synthetic, polypropylene fibers were examined along with three different interface preparation methods on the hybrid specimens. It was determined that using a blended macro-micro fiber provided the best results in terms of toughness before and after flexural cracking. Results also indicated that using an intentionally roughened surface similar to roadway tines resulted in the best flexural performance compared to the other surface preparation methods in this thesis. FRC beams provided the best flexural performance out of the three sections evaluated, but a hybrid section provided double the flexural performance of an unreinforced, PC section.

Acknowledgements

First and foremost, I would like to thank Alan Meadors and the American Concrete Pavement Association (ACPA) and Weaver-Bailey Contractors for their invaluable financial support of this research. Their willingness to fund research projects and invest in the further education of students, like myself, cannot be appreciated enough.

I want to extend my heartfelt gratitude and appreciation to my graduate advisor, Dr. Cameron Murray, for giving me this opportunity and for the countless hours of mentorship, guidance, and encouragement during my graduate studies.

I could not have accomplished the countless hours of lab work without the help of Bette Poblete, Rilye Dillard, Caleb Chestnut, Behzad Farivar, David Peachee, and Mark Kuss. I would also like to thank Bette and Rilye for their help during the drafting and editing process of this thesis.

I want to give special thanks to my parents, Laura and Dewayne Keys, for their continued prayers, support and guidance throughout this journey and for constantly keeping me motivated and focused.

Last, but certainly not least, I would like to acknowledge my Heavenly Father who gave me the wisdom and strength to accomplish this task, at a great university, with great professors, a great advisor, and great friends.

Table of Contents

1. Introduction

FRC provides many benefits compared to unreinforced, plain concrete (PC) including increased ductility and toughness, increased flexural strength in high doses of fiber (around 4%), increased impact resistance, and increased tensile capacity, among many others [1], [2]. One major disadvantage of FRC is that it can lead to challenges in achieving an acceptable surface finish, especially if a special finish such as roadway tines is required. While there may be other options to finish a FRC surface to reduce dragging the fibers such as reducing the tining angle or grinding the grooves after concrete hardening [1], another option is to maintain a PC layer at the top of the pavement section. The purpose of the research reported in this thesis was to create a hybrid PC – FRC section that could combine the strength and crack control benefits of fibers with the ease of finishing of PC.

Concrete pavements exhibit two different types of cracking: longitudinal cracking (along the length of the pavement) and transverse cracking (along the width of the pavement). There are many reasons that concrete will crack longitudinally, but the three main reasons are due to: poor subbase and subgrade that allows for settlement cracks, issues during construction regarding saw cut joints and improper dowel placement at the joints causing cracking, and aggregates with higher thermal expansion causing more internal cracking in the concrete [3]. Transverse cracking can be caused by flexural loading (the focus of the study in this paper), but it is also created throughout the concrete by shrinkage of the concrete expanding and contracting. Without reinforcement, the only forces resisting these cracks are the friction forces between the aggregate in the concrete referred to as “Aggregate Interlock” [4].

Only synthetic fiber reinforcement was used in the FRC in this study. Synthetic fibers are man-made fibers that are made up of different polymer types. The study presented in this thesis dealt with polypropylene and polyethylene polymers. Smaller synthetic fibers are useful for controlling thermal cracking due to their low coefficient of thermal expansion, and larger synthetic fibers are sufficient substitutes for steel fibers due to their corrosion resistance [1]. In this work, the performance of a hybrid section of pavement, that is a layer of PC on top, and a FRC layer below was compared to the performance of FRC and PC beams. Surface preparation methods between the layers were also evaluated to provide a full understanding of what would provide the best results if this type of pavement section was to be adopted in future concrete pavement construction. This proposed hybrid section was evaluated using hybrid concrete beam specimens and comparing them to PC beams and FRC beams. To compare the effectiveness of hybrid specimens to FRC and PC specimens, flexural tests were performed since the loads on pavements often result in flexural stresses. The bond between the layers was also evaluated using slant shear cylinder specimens.

2. Background

2.1 Portland Cement Concrete Pavements

The first Portland Cement Concrete (PCC) pavement constructed in the United States was in Bellefontaine, OH in 1891. This pavement was actually two layers of PCC pavement, referred to as a PCC/PCC composite pavement. The top layer was a 4 in. thick structural layer with no special aggregates, whereas the bottom layer was a concrete layer consisting of a more durable aggregate type [5]. Since then, engineers and builders have strived to optimize and find the perfect concrete pavement. According

to the Portland Cement Association (PCA), there are four different types of concrete pavements: a PC pavement with reinforcing dowels to provide load transfer, a PC pavement without dowels, a jointed reinforced concrete pavement with steel reinforcement in the joints, and continuously reinforced concrete pavements which have no contraction joints and contain continuous longitudinal reinforcement throughout their length. All methods of creating joints in concrete are to control transverse and longitudinal cracking and movement of the concrete. A concrete pavement with joints will still crack, but the idea is for the crack to form below the joints instead of on the surface of the concrete. Reinforcing bars (dowels) at the joints hold these joints together and prevent excessive long-term cracking. However, transverse cracks may also form throughout the concrete at places other than the joints. This can be mitigated by adding longitudinal steel reinforcement throughout the pavement section between joints. Therefore, a pavement with dowel bars in the joints and no longitudinal reinforcement will have good crack control at the joints, but it could still have excessive cracking between the joints in the pavement section [6], [7]. Another approach to provide continuous reinforcement in concrete pavements is to add fiber reinforcement to the concrete mix design to ensure that there is crack mitigation throughout the concrete.

2.2 Fiber Reinforcement in Concrete

In the early 1960's, fiber reinforcement became an alternative to conventional steel reinforcement. Since the 1960's, steel fibers, glass fibers, synthetic fibers, and natural (cellulose) fibers have been studied extensively in different applications. Fiber dosages in the range of 0.1 to 1.0% were classified as a low dosage, a fiber dosage in the range of 1.0 to 3.0% was classified as a moderate dosage, and a dosage range of

3.0 to 12.0% was classified as a high dosage [8]. The fibers used in the study reported in this thesis were synthetic, polypropylene macrofibers and are discussed in more detail in Section 3.1.1. The Fiber Reinforced Concrete Association (FRCA) delineates macrofibers and microfibers by their equivalent diameter and linear density. Microfibers have an equivalent diameter less than 0.012 in. and a linear density of less than 1.28 lbs. / 5.59 mi. of fiber. Macrofibers have an equivalent diameter greater than or equal to 0.012 in. and a linear density greater than or equal to 1.28 lbs. / 5.59 mi of fiber [9]. Since macrofibers are larger, they typically are better suited for structural applications and load carrying situations, while microfibers are more effective at reducing temperature and shrinkage cracking [10].

A study at the University of Tennessee evaluated the effects of six different fiber types including steel, glass, and carbon fibers, and varied fiber dosages from 0.3% to 1.0% by concrete volume. This study evaluated fresh concrete properties such as slump flow, and also hardened properties like early-age compressive and flexural strengths. The study concluded that specimens including a steel fiber dosage of 1.0% provided the highest 6 hour strengths and good workability [11].

Another study evaluated the flexural performance of a hybrid section of fiber reinforced polymer (FRP) rebar and polypropylene fibers. The study used 0.5 in. and 1.0 in. diameter FRP bars and a fiber dosage of 0.5% for the polypropylene fibers. The study compared these FRC beams to PC beams under a four-point bending configuration and compared the crack widths during testing. It was concluded that the FRC beams had 40% more ductility than the PC beams, and smaller crack widths than the PC beams [12].

A study at Wuhan University in China evaluated the tensile capacity of hybrid steel and polypropylene FRC specimens using dosages of each fiber type up to 1.9%. Testing was conducted using a uniaxial tensile test, and the results showed that using a mixture of fiber types in a concrete specimen can increase the tensile capacity by 25% to 80% when compared to PC [13].

A study involving cellulose fibers (fibers made from wood) evaluated many properties of their FRC specimens and compared them with specimens made from polypropylene fibers. The study evaluated multiple forms of shrinkage, compressive strengths, toughness, flexural strengths, and modulus of elasticity. The researchers determined the following about the addition of fibers: shrinkage control was increased, 28-day compressive strengths were unaffected as well as flexural strengths and modulus of elasticity results, but the toughness of the FRC specimens were 40% to 90% higher than the PC specimens. The study also determined that cellulose fibers provided the same results as polypropylene fibers in similar doses, and that the cellulose fibers were actually the cheaper option [14].

Researchers at Iowa State University investigated the effects of 4 different dosages of carbon microfiber (0%, 0.1%, 0.3%, 0.5%). Shrinkage effects were evaluated along with compressive strength tests and splitting tensile strength tests. The study concluded that increasing the fiber dosage increased the compressive strength at early ages, and increasing the fiber dosage also increased the tensile strength and crack resistance of the concrete [15].

A study in Eastern Europe investigated the effects of composite carbon and glass macrofibers at a dosage of 1.5%. Compressive strengths were evaluated, fiber pullout

was evaluated, and four-point bending tests were conducted. The study found that the compressive strength was dependent on the w/c ratio instead of the fibers, that fiber pullout strength is dependent upon the orientation of fibers in the concrete, and that composite fibers had worse flexural performance than steel fibers at the same dosage [16].

Two relevant studies were found that examined FRC specifically for a pavement application. The first of which was a study in Florida that examined the performance of FRC for use as a concrete pavement slab replacement. The study focused on the early stages of FRC since pavement repairs need to be operational shortly after construction. The results of the study showed that short (0.5 to 1.0 in.) polypropylene fibers performed the best at resisting early-age cracking, and as a whole, the use of fiber reinforcement in concrete increased early age cracking resistance and thus, early age strength [17]. The other study, performed in Minnesota, evaluated the performance of FRC for thin concrete pavements and overlay applications. The results of this study showed that transverse joint faulting decreased with an increase in fiber dosage [18]. Joint faulting in pavement refers to the vertical deflections at the joints which affects the smoothness of the ride [19].

Studies have also been performed to evaluate the effectiveness of FRC pavement applications in the field. One such study in Italy, monitored a polypropylene based FRC pavement after construction under traffic conditions. Over a four-month period, the study concluded that the internal longitudinal and transverse strains of the pavement were similar to before loading was applied [20]. Another study focused on the effectiveness of using synthetic fibers for reinforcement in airport concrete pavement.

The study found that the addition of synthetic fibers can reduce concrete permeability and improve concrete frost resistance. The study also performed a cost-benefit analysis and concluded that the optimum synthetic fiber dosage for airport concrete pavements was 0.10 to 0.14% of the concrete volume [21].

2.3 Hybrid PC and FRC Concrete

During literature review, only one other study proposed a hybrid concrete section of PC and FRC, and this hybrid section was compared with PC control sections. A study in Germany proposed a hybrid concrete section to mitigate the effects of large tensile stresses at the top of the member due to concentrated loading. This region at the top of the concrete specimen was referred to as the “St. Venant disturbance zone”. The specimens in this study were columns in compression loading. Steel fibers were added to this St. Venant disturbance zone, and the FRC layer was varied to determine the optimum layer depth. Surface preparation methods were not analyzed. Instead, the two layers of concrete were bonded by a method referred to as a “’wet-on-wet’ casting technique” in which both of the layers were still wet when they bonded to each other. The results of this study showed that increasing the layer of FRC increased the maximum bearing capacity of the hybrid sections, and that the hybrid sections had significantly more “post-cracking ductility” than the PC sections [22].

3. Materials and Methods

3.1 Materials

3.1.1 Fiber Types

Four fiber types were evaluated during the testing described in this thesis. These fiber types included macrofibers and a blend of macro and microfibers. During testing, test specimens containing each fiber were described as “Fiber #”. This notation will be used throughout this thesis. Figure 1 provides a visual comparison of all four fiber types. Some of the fiber types were easily separated into smaller threads, whereas others were singular strands of fibers. Some engineering properties for the fibers are given in Table 1. Note that some of the engineering properties were not available for fibers 1 and 4, since this company did not perform extensive lab testing on their fibers.

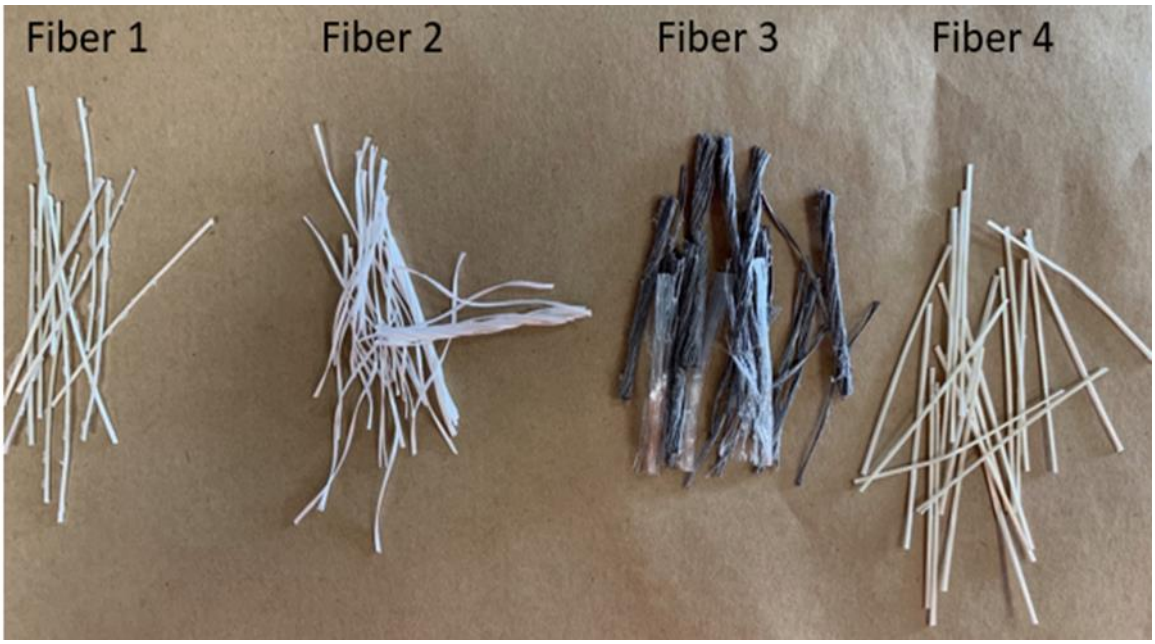

Figure 1. Visual comparison of all four fiber types.

Fiber 1 was individual strands of polyamide macrofibers. Polyamides are nylon polymers that are well known for maintaining their mechanical properties at higher temperatures [23]. According to the manufacturer, this fiber also had a coating on the surface designed to bond with the cement paste during curing and was designed specifically for members that experience impact loading [24]. Although no impact loading was conducted during this research, flexural strength was evaluated. These fibers were rigid compared with the other fibers in this study and had a rough surface and approximate dimensions of 0.03-0.04 in. in diameter and 2 in. in length.

Fiber 2 was a polypropylene and polyethylene synthetic macrofiber. These macrofibers consisted of smaller strands spun into a larger strand. These larger strands unraveled upon mixing resulting in a thorough dispersion of the smaller fibers in the concrete. The diameter of the larger strand was approximately 0.1 in. and the diameter of the smaller strands was approximately 0.05 in. These strands were approximately 2 in. in length. Similar to Fiber 1, these fibers were rigid.

Fiber 3 was a mixture of two fiber types: a standard polypropylene microfiber for resisting temperature and shrinkage cracking, and a heavy-duty monofilament macrofiber for improved strength [25]. The monofilament strand consisted of smaller fiber strands similar to Fiber 2. The diameter of the larger fiber was approximately 0.01 in., and the diameter of the smaller fiber was approximately 0.075-0.1 in. The lengths of these strands were approximately 2.25 in.

Fiber 4 was designed to be used in precast concrete members [26]. These fibers were similar to Fiber 1, although they were not as rigid and were more lightweight in

comparison. The diameter of this fiber was approximately 0.025 in., and the length was approximately 2.5 in.

Table 1. Engineering properties of fibers.

	Specific Gravity	Tensile Strength (ksi)
Fiber 1	N/A	N/A
Fiber 2	0.92	87-94
Fiber 3	0.91	83-96
Fiber 4	1.16	N/A

Note: All data was gathered from manufacturer documents [24]–[27]

3.1.2 Concrete Mixture Materials

All concrete mixtures and materials conformed to Arkansas Highway and Transportation Department (AHTD) Specification Section 501, Portland Cement Concrete Pavement Requirements [28]. The cement used in the concrete mixtures was a standard Type I/II portland cement. The coarse aggregate used in all of the concrete mixtures was a 1-inch nominal maximum size, number 57 crushed limestone. The gradation, specific gravity (SG), and absorption of the coarse aggregate used in the concrete mixtures are shown in Table 2. The fine aggregate used in the concrete mixtures was Arkansas river sand from Van Buren, Arkansas. The gradation, fineness modulus (FM), SG, and absorption values for the fine aggregate are shown in Table 3.

Table 2. Course aggregate properties.

Sieve Size	Retained (%)	Passing (%)
1 1/2	0	100
1	0	100
3/4	10.26	89.74
1/2	33.32	66.68
3/8	49.91	50.09
4	83.35	16.65
8	94.61	5.39
16	95.98	4.02
30	96.31	3.69
50	96.54	3.46
100	96.76	3.24
200	97.04	2.96
Pan	97.13	2.87
Specific Gravity		2.565
Absorption (%)		2.4

Table 3. Fine aggregate properties.

Sieve Size	Retained (%)	Passing (%)
3/8	0.0	100.0
4	2.8	97.2
8	8.1	91.9
16	19.5	80.5
30	39.0	61.0
50	83.2	16.8
100	97.9	2.1
200	99.3	0.7
Pan	99.4	0.6
Fineness Modulus		2.51
Specific Gravity		2.63
Absorption (%)		0.55

To ensure adequate workability, AdvaCast 575 was used as a high-range water reducer (HRWR) for all mixture designs. This HRWR is a polycarboxylate based formulation. Terapave air-entraining agent (AEA) was also added to the concrete mixtures to ensure compliance with the 2014 AHTD Specification Section 501.

Terapave is an acid salt-based air entrainer. This section specifies that air content of the fresh concrete be 6% ± 2% (4-8%) [28].

3.2 Mix Designs

For the mixtures that contained fiber, a constant dose of 10 pounds per cubic yard, approximately 0.26% by concrete volume, of fiber was used. It was observed that the air content was high in early batches, so the AEA dosage was reduced and kept constant thereafter. The HRWR dosage was adjusted to provide adequate workability for the mixtures while changing fiber types. In this case, adequate workability was defined as a 2-to-3-in. slump. The admixture dosages ranged from 0.5 to 3.0 fl. oz of HRWR and 0.5 to 1.0 fl. oz of AEA for all the concrete mixture designs. A summary of the mixture design is shown in Table 4.

Table 4. Mixture design for concrete.

Mix Design	Weight (lb/CY)
Cement	611
Sand	1264
Rock	1691
Water	257
Fiber	10

3.3 Methods

3.1 Concrete Mixing Process

To conform to ASTM C192, all concrete mixture materials were added to a revolving drum mixer as follows: coarse aggregate, half the water (at this point the mixer was turned on), fine aggregate, cement, and the rest of the water [29]. The first half of water contained the HRWR, and the second half of the water contained the AEA. Both

admixtures were added to the mixing water immediately prior to mixing the concrete. The concrete was mixed for 3 minutes after all materials were added. After initial mixing, the mixer was then turned off for 3 minutes to allow the concrete to rest. After allowing the concrete to rest, the concrete was mixed for a final 2 minutes. The concrete mixing process for the FRC was the same for that of the PC except for the addition of fibers. The fibers were added before the mixer was started at the same time that the coarse aggregate was placed in the drum. Adding the fibers in this manner ensured adequate dispersion throughout the concrete during mixing by allowing it to mix for the whole duration.

3.3.2 Specimen Casting Procedure

Five different types of specimens were cast from these concrete mixtures: standard concrete cylinders, “hybrid” slant-shear cylinders, “hybrid” PC and FRC beams, FRC beams, and PC beams. “Hybrid” refers to a concrete beam with two concrete layers and, therefore, two separate concrete mixtures. The bottom layer was FRC, and then a PC top layer was added. Each bottom layer cured for at least 7 days before the PC was placed on top. Some top layers were placed more than 7 days apart. For example, Fiber 1 hybrid specimens were cast 11 days apart due to slump issues with the planned top layer. Fiber 4 specimens were cast 8 days apart because day 7 fell on a holiday. A seven-day minimum was chosen to allow the bottom layer to gain strength before the addition of the second layer and as a representation of how this concrete section might be done in the field. Theoretically after 7-days, the mixture had adequate strength to have construction loads applied to it. Three different surface preparations were used on the hybrid slant shear test specimens and the hybrid beam

test specimens to determine a method that would provide the best interface bonding preparation for field applications. One was a control method with no surface preparation, another was to expose aggregate at the interface surface, and the last method mimicked roadway tines.

In the first surface preparation method, the surface was struck off to provide a smooth finish, but no extra finishing was performed. This was to serve as the base comparison for the other two methods. This was marked as “None” on specimens. Examples of this method are shown in Figure 2.

Figure 2. No surface preparation method for slant shear cylinders (left) and beams (right).

The second surface preparation method utilized a set retarder. The set retarder used in this research was MasterSet DELVO. DELVO is a Type B set retarding admixture conforming to ASTM C494 [30]. It was applied to the top surface by spray bottle immediately after casting and then, 24 to 48 hours after curing, the top layer of

paste was removed with a wire brush attached to an electric grinder. This provided a rough, exposed aggregate surface for the overlay to bond to. It also exposed fibers in the base layer that may have provided additional bonding. This preparation method was marked as “DELVO” on specimens. Examples of this surface preparation are shown in Figure 3.

Figure 3. Example of DELVO surface preparation method for slant-shear cylinders (left) and beams (right).

The last surface preparation method used was intended to mimic roadway tines. Often, concrete roadways are tined longitudinally to improve safety and reduce noise [31]. The hybrid beams and slant shear cylinders were tined in this way with a handheld device that conforms to the specifications in AHTD Section 501 [28]. This surface preparation method was difficult to perform due to the dispersed fibers being very close to the top of the finished surface. When the tining device was dragged along the top surface of the concrete it resulted in snagging fibers and dragging them along the

surface, marring it. It was especially difficult on the slant-shear cylinders due to the geometry on the top surface of the slanted cylinder molds. This surface preparation method was marked as “Tines” on all test specimens. An example of specimens prepared by this method is shown in Figure 4.

Figure 4. Example of tines surface preparation method for slant-shear cylinders (left) and beams (right).

3.3.2.1 Compression Test Specimens

Nine standard 4 in. by 8 in. concrete cylinders were cast with every mix. Three cylinders each were cast for one day, 7-day, and 28-day compressive strength testing. All cylinders were cast according to ASTM C192/C192M [29]**.**

3.3.2.2 Slant Shear Test Specimens

Nine total hybrid slant-shear cylinders were cast for each fiber type, 3 for each surface preparation, to test the bond strength (in shear) of each of the surface

preparation methods. The cylinders were tested 28 days after the top layer was cast. A pure compression failure (cracks propagating through the boundary interface) was considered good bond, and a pure shear failure (failure along the boundary interface) was considered a bond failure. This analysis aligns with similar research using slant-shear specimens [32].

First, a base FRC mixture filled the cylinders halfway up. Next, a batch of PC was made to fill the cylinders to the top. The cylinder holder was made at a 45-degree angle so the interface between the FRC, and PC was at a 45-degree angle. After the first layer was cast, the cylinders were left to cure where they were cast – inside a room at approximately 75ºF until the PC surface layer was placed. Once the cylinders were cast with the first layer, they were not moved to ensure that the concrete cured as close to a 45-degree surface interface angle as possible. To place the top PC layer, the partially filled cylinder molds were placed on the ground normally and filled to the top. The special cylinder holder is shown in Figure 5. Demolded slant-shear cylinders are shown in Figure 6, showing the 45-degree bonded interface.

Figure 5. Formwork for slant-shear cylinders.

Figure 6. Slant-shear cylinders after demolding.

All slant-shear cylinders were consolidated by a combination of rodding with a 3/8” diameter rod and using a small electric concrete vibrator. Without using a vibrator, it was very difficult to consolidate the overlay mixture onto the slanted fiber mixture and get a good bond between the two layers. This was due to the slanted surface and space constraints in the cylinder mold along the edge of the existing concrete. Proper consolidation the original set of slant shear cylinders was not achieved for the first two fiber types. These slant-shear cylinders were repeated at a later date using the same mixture design to achieve more consistent results.

3.3.2.3 Beam Test Specimens

Three different preparations of beam test specimens were made for each fiber type. Three full FRC beams were made, three PC beams were made, and six hybrid PC and FRC beams were made for each fiber type. First, an FRC mixture was made and was used to make compressive strength cylinders, full-FRC beams and the bottom layer of the hybrid beams. Next, a batch of PC was made and used to make control PC beams, control PC compressive strength cylinders, and to finish casting the hybrid beams. Of the six hybrid beams, two beams were cast for each surface preparation method. In total, twelve beams were made for each fiber type and 48 total beams were made. Each beam was 6 in. wide, 6 in. deep, and 21 in. long.

The FRC and PC beams were cast as normal beams in a metal mold. However, the hybrid beams were cast in plastic molds with a special configuration for the third point loading points. In order to guarantee a flat surface for the third-point loads, metal plates were placed on top of the plastic mold and were held down by clamps. The concrete was then cast under the metal plates to ensure a flat surface. After removal of

the metal plates, air voids under the plates were filled with a fast-setting cement paste and the surface was struck off with a putty knife. This was to ensure that no air voids existed where the load points would be located. The molds for the hybrid beams are shown in Figure 7. All beams were cast according to ASTM C192/C192M [29].The ASTM suggests using a rod to consolidate concrete within these molds, but since the concrete was relatively low slump (2 to 3 in.), an electric vibrator was used to consolidate the concrete.

Figure 7. Formwork for hybrid beams.

3.3.3 Specimen Breaking Procedures

3.3.3.1 Testing Procedures for Compression Test Specimens

All samples were stored in a lab environment for the first day after casting. The next day, all cylinders were demolded, the one-day breaks were performed, and the other cylinders were stored in an environmental chamber at a temperature of approximately 73ºF and relative humidity of approximately 50% until it was time to test

them. The FRC cylinders were trimmed with scissors before they were put in the grinder for neatness. An example of the cylinders before and after trimming is shown in Figure 8. Before the cylinders were tested, both sides were grinded to a plane and smooth surface using a concrete cylinder grinder (shown in Figure 9). The cylinders were then tested in a Forney VFD compression machine according to ASTM C39/C39M [33]. The break load was recorded and then used to calculate the compressive stress of the cylinder. The Forney VFD system is shown in Figure 10.

Figure 8. Fiber cylinder before trimming (left) and after trimming (right)

Figure 9. Grinder for cylinders.

Figure 10. Forney compression frame.

3.3.3.2 Testing Procedures for Slant Shear Test Specimens

The ASTM for slant shear specimens (ASTM C882/C882M) was loosely used to perform the bond strength tests in this study [34]. The slant shear and standard compression cylinders were tested identically. The same loading rates were used as in ASTM C39 [33].

3.3.3.3 Testing Procedures for Beam Test Specimens

The beams were tested under a third point loading configuration. The goal of these tests was to evaluate the flexural cracking of these test specimens. Third point loading setup provides constant flexural stress in the middle third of the specimen. A third point loading frame was attached to an MTS servo-hydraulic universal testing machine to apply the desired loading configuration and to provide load and midspan deflection values. To avoid excessive deflections at the supports and provide stiffness, a 6-inch-deep wide flange shape was placed underneath the third point loading frame. The testing configuration for all beams is shown in Figure 11. All beams were tested according to ASTM C1609/C1609M [35]. Even though some beams did not have fiber reinforcement in them, they were tested according to the ASTM referring to fibers to conform to the same loading rates across all specimen types.

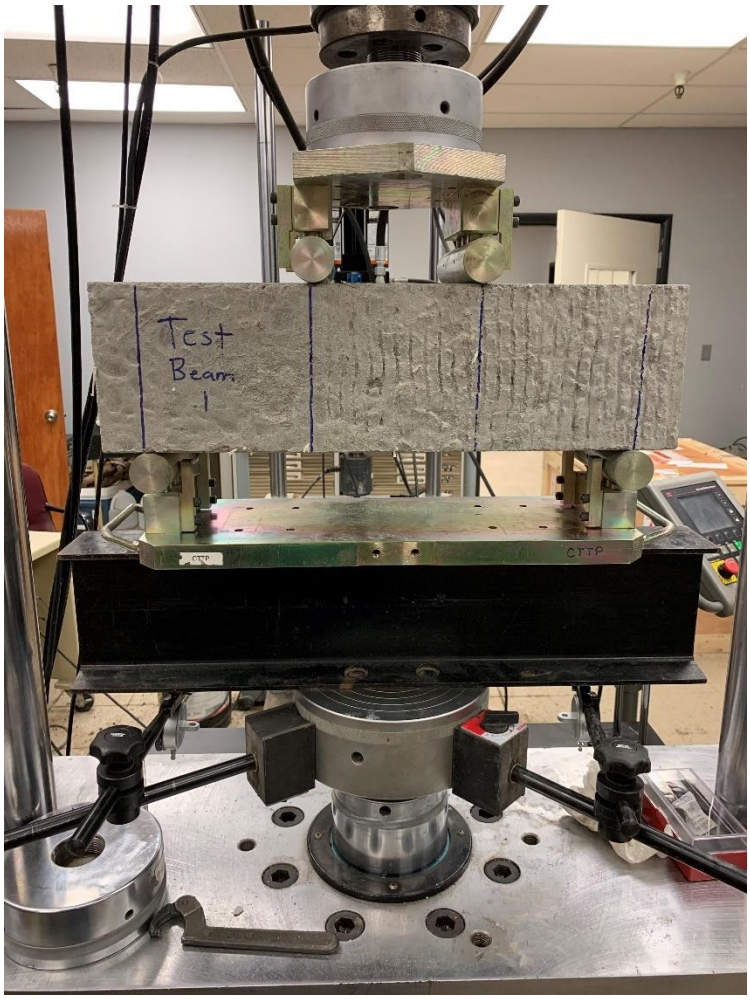

Figure 11. Third point load frame for beam testing.

Deflections and loads were measured by the MTS system, and the deflection was the midpoint deflection measured at the ram. Three loading rates were applied to all beams during testing: 0.0035 in./min. up to a deflection of 0.02 in., 0.012 in./min. after a deflection of 0.02 in. until 0.12 in., and then a loading rate of 0.06 in./min. until the end of test. ASTM C1609 specifies the end of test is at a deflection of 0.12 inches [35]. However, testing was continued to a deflection of 5 to 6 times the value specified in ASTM 1609 to observe trends in the load vs. deflection curves discussed later. Two different loading rates were required per ASTM [35], but the third loading rate was a

custom rate intended to decrease the total testing duration and continue loading the beams to large deflections. The load vs. deflection data was then captured at a frequency of 1 Hz (1 data point every 1.0 second) in order to develop load vs. deflection curves for each beam. After the end of the test, the width and depth of each beam was measured to calculate modulus of rupture per ASTM C1609 [35].

4. Results

4.1 Description of Fresh Properties

For each mix, five different fresh concrete properties were recorded. Ambient temperature (ºF), water temperature (ºF), concrete mixture temperature (ºF), slump (in.), and air content (%) were all measured to ensure consistency between batches. As stated previously, the target slump was 2-4 in., the target air content range was 4-8% and the target concrete mixture temperature was 70ºF. Table 5 shows the fresh concrete properties for all mixes. As shown in Table 5, the water temperature was adjusted according to the ambient temperature to keep the mix temperatures consistent. The variation in ambient temperatures is a result of performing mixes outside. All mixtures occurred between the months of March and June and varied in the time of day. Despite these variations, the mixture temperatures were all similar and all the slump and air content values fell within the targeted ranges. All mixtures were consistent with pavement concrete in the field.

Table 5. Fresh properties for all mixes.

Mix Name	Water Temperature (ºF)	Ambient Temperature (ºF)	Mixture Temperature (ºF)	Slump (in.)	Air Content (%)
FRC1	80.2	70.5	74.1	3.0	7.8
PC1	74.1	57.0	69.8	3.5	8.0
FRC2	65.9	63.3	70.5	1.5	5.3
PC2	66.0	75.2	75.0	3.0	6.0
FRC3	68.7	47.8	69.4	1.0	4.5
PC3	72.1	66.6	73.4	2.0	4.7
FRC4	73.2	65.3	73.2	2.0	4.5
PC4	66.6	58.1	68.4	2.0	5.9

Note: FRC = Fiber Reinforced Concrete, PC = Plain Concrete.

4.2 Compression Test Specimen Results

Standard compressive strength cylinders were tested at 1-day, 7-days, and 28-days. The 7-day strengths of the FRC were measured on the same day the top layer of PC was cast on top of the beams. This 7-day strength may be relevant to field applications of hybrid sections, as it provides an estimate to the strength of the bottom layer, specifically if it could support equipment to pour the top layer of the hybrid section. All cylinder compressive strengths are shown in Table 6. All 28-day strengths met the required 4000 psi compressive strength outlined by AHTD Section 501 [28].

Table 6. Compressive strengths for 1-day, 7-day, and 28-day cylinders.

Mix Name	Avg. 1-day Compressive Strength (psi)	Avg. 7-day Compressive Strength (psi)	Avg. 28-day Compressive Strength (psi)
FRC1	1,500	3,740	4,370
PC1	2,270	4,060	4,440
FRC2	2,180	4,110	5,400
PC2	2,720	4,770	5,630
FRC3	3,170	5,460	6,160
PC3	3,030	5,400	5,760
FRC4	3,350	5,980	6,530
PC4	2,900	4,670	5,480

When examining the 1-day compressive strengths from Table 6, one can notice an average strength of 2,550 psi for the FRC cylinders and 2,730 psi for the PC cylinders. When looking at the 7-day compressive strengths, one obtains an average strength of 4,820 psi for the FRC cylinders and 4,725 psi for the PC cylinders. Lastly, the averages for the 28-day compressive strengths were 5,615 psi for the FRC cylinders and 5,330 psi for the PC cylinders. Therefore, the cylinder strengths were roughly similar when comparing the PC and FRC cylinders. The differences in the slant shear cylinders discussed in Section 4.3 can be attributed to the effects of the concrete at the interface.

4.3 Slant-Shear Test Specimen Results

Slant shear cylinders were tested at 28-days to correspond with their respective beam breaks. The purpose of the slant shear cylinders was to directly observe the effect of surface preparation methods on the bond strength. That is, if the cylinders failed in the base material(s) it was considered a good bond, whereas if they failed along the interface between the two materials the bond was considered to be poor. An illustration of these failure types is shown in Figure 12. The goal was to determine which surface preparation method provided the best bond.

Figure 12. Failure in base materials (left) and shear failure at boundary interface (right).

All slant shear specimen results are shown in Table 7. Each row in Table 7 is an average of three cylinders prepared from the same mixtures. The slant shear break data shown in Table 7 allows more direct comparison of the surface preparations than the prism tests. A comparison between fiber types and surface preparation methods is also shown in Figure 13. There was a clear difference in strengths between the surface preparation types. Across all the fiber types, the cylinders with no surface preparation achieved the highest strengths, followed by the cylinders that were tined. The DELVO cylinders consistently had the lowest strength. The second conclusion from this data is that all the methods except for the DELVO method led to failures in the base material, and thus by the criterion established previously, can be concluded as surface preparation methods that provide a good shear bond between layers of concrete. The shear failures along the boundary interface of the DELVO cylinders could be a result of the wire brush not effectively removing the top surface of paste because the cylinders were at an angle when the DELVO method was performed. This implies that the top

layer of concrete bonded to a layer of paste that was not properly set or connected to the bottom layer of concrete, i.e. the shear key was not developed. A “shear key” refers to an element added between layers of structural material, in our case, the grooves with the tines method, to provide good shear resistance between the surfaces. If some form of grip is not achieved between layers, there will likely be a bond failure as shown in this case. Recall that DELVO was a set retarder so the addition of DELVO might have weakened the concrete in the bottom layer by preventing it to fully cure.

Table 7. Slant shear cylinder break data.

Name	Avg. Stress (psi)	Failure Type
H1N	5,084	Base Failure
H1D	2,995	Interface Failure
H1T	4,643	Base Failure
H2N	5,185	Base Failure
H2D	3,369	Interface Failure
H2T	5,004	Base Failure
H3N	7,078	Base Failure
H3D	5,096	Interface Failure
H3T	5,915	Base Failure
H4N	6,412	Base Failure
H4D	4,109	Interface Failure
H4T	5,911	Base Failure

Note: “H1N” = Hybrid, Fiber 1 None, “H1D” = Hybrid, Fiber 1 DELVO, etc.

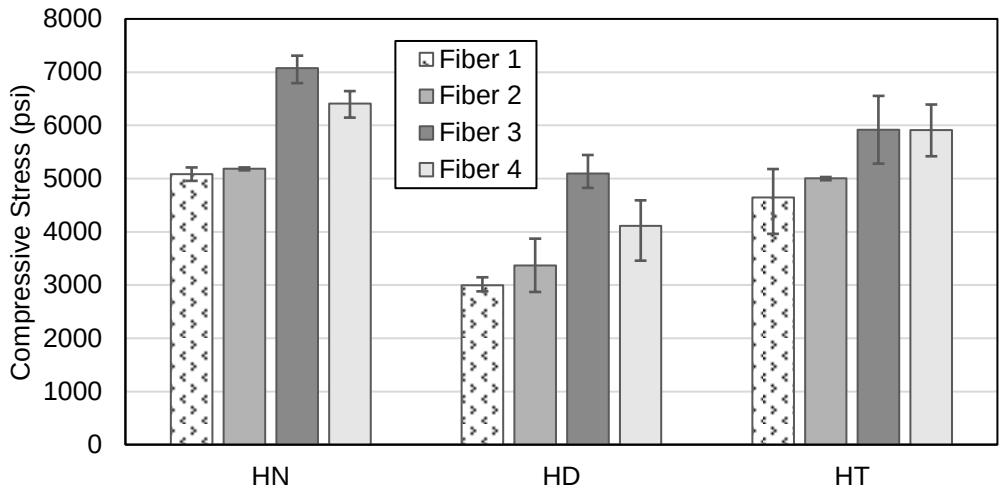

Figure 13. Comparison of slant shear cylinders.

4.4 Beam Test Results

4.4.1 PC Beam Test Results

In a PC flexural strength test, the beam fails completely after the first flexural crack forms. An example of this behavior from this research is shown in Figure 14. The lines drawn on the beam indicate the third point locations. A crack/failure forming in between the middle third is the objective with this type of loading configuration. This is the region of constant moment with no shear. This type of failure was consistent across all PC beam breaks. This failure results in a load vs. deflection curve with a linear trend up to the cracking load followed by a complete loss of strength. This is shown by all PC beam failures in Figure 15. The initial portion of these curves is non-linear and resulted from initial settling of the loading device. In Figure 15, all PC beams were grouped by color and line texture. For example, PC1 and PC2 were beams made from the first batch, and PC3, PC4, and PC5 were beams made from the second batch. Only two beams were included from the first batch because of an error during preloading one of the beams. All beams achieved failure before a deflection of 0.06 in., and all beams

experienced failure at similar loading (6,000 to 6,500 pounds) except for PC9, PC10, and PC11, which experienced failures at loads of approximately 8,000 pounds. The cause for this increased flexural strength in the fourth batch of beams is unknown, given its similar compressive strength, air content, and curing to other beams. Other than this increase in failure load, the load vs. deflection curves for all of the PC beams made in this research were similar.

Figure 14. Typical failure of a PC beam.

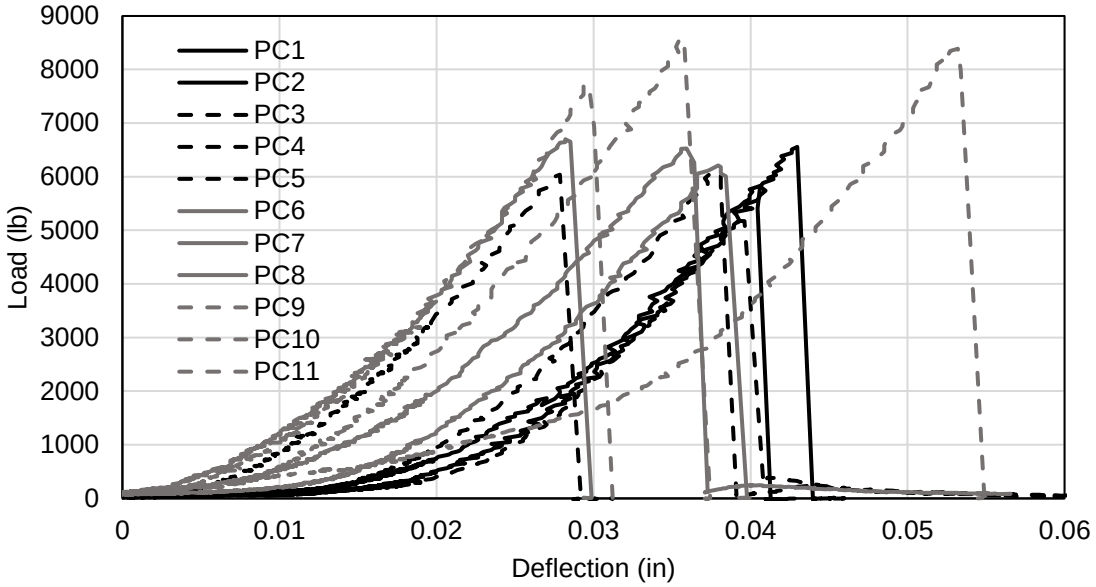

Figure 15. Load vs. deflection curves for all PC beams.

4.4.2 FRC Beam Test Results

Compared to PC, the FRC beams in this research were found to fail in a slow and ductile manner. Generally, the behavior of these beams was characterized by a first peak load when the first flexural crack appeared, a drop in load, then a strain hardening response up to a second peak followed by strain softening. This strain hardening and strain softening behavior in FRC is more thoroughly discussed in a study performed in Italy and Japan [36]. Once the FRC beams reached their peak loads and initial cracks started to form, they continued to carry load and gradually deflect in a ductile manner. In most cases, many fiber strands were observed bridging the widening crack. An illustration of a full FRC beam at the end of testing is shown in Figure 16.

Figure 16. FRC beam at end of test.

Figure 17 shows the load vs. deflection curves for all the FRC beams made with Fiber 1. In some of the Fiber 1 load vs. deflection curves there are increasing and then sharply decreasing loads after the second peak. This was caused by individual fiber strands or strand groups engaging and failing. This engagement and failure of the fiber strands can be observed by the zig-zag part at the end of the curve for FC1 - Beam 2 in Figure 17. The FRC beams did not break completely in two halves like the PC beams illustrated in Figure 14. In many cases, the FRC beam halves were still connected after failure, and they were separated with a mallet after the loading process was completed to measure the cross-sectional dimensions at the failure location. The FRC beams for Fiber 1 were only tested up to a deflection of approximately 0.14 in. This is because the test can be terminated at a deflection of 0.12 in. per ASTM C1609/C1609M [35]. However, it was decided to continue loading other fiber types longer in case a trend in the load vs. deflection curves was missed at these larger deflections. All beams for

Fiber 1 cracked within the middle third and cracked at an average peak load of 6,200 pounds for the FRC beam set. One of the FRC beams tested with Fiber 1 is shown in Figure 18.

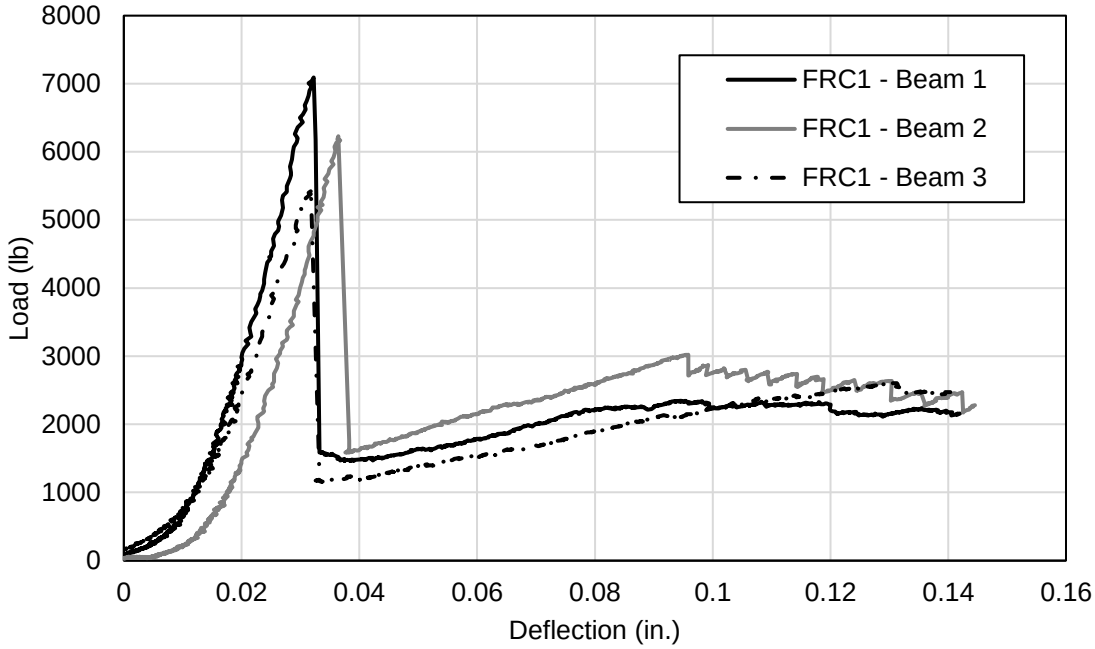

Figure 17. Load vs. deflection curves for Fiber 1 FRC beams.

Figure 18. Fiber 1 FRC beam at end of test.

All the load vs. deflection curves for the Fiber 2 FRC beams are shown in Figure 19. Fiber 2 beams, which were loaded for a longer period of time than the Fiber 1 beams, clearly depicts a first peak load followed by an incomplete loss of strength, strain hardening, and then strain softening. These FRC beams initially cracked at a deflection around 0.05 in. (similar to Fiber 1) and then experienced strain hardening up until a deflection of approximately 0.15 to 0.2 in. After this point, they underwent strain softening and gradually lost strength as each fiber strand that was engaged began to fail. All three of these beams initially cracked within the middle third with the first peak load averaging approximately 6,750 pounds. An example of an FRC beam break from Fiber 2 is shown in Figure 20.

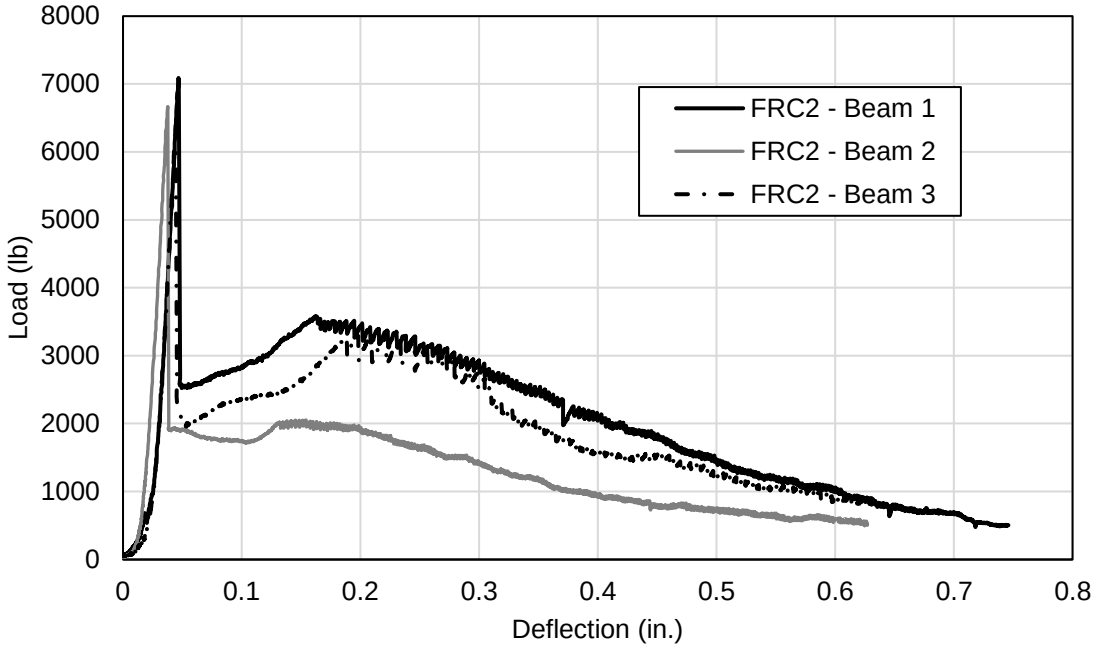

Figure 19. Load vs. deflection curves for Fiber 2 FRC beams.

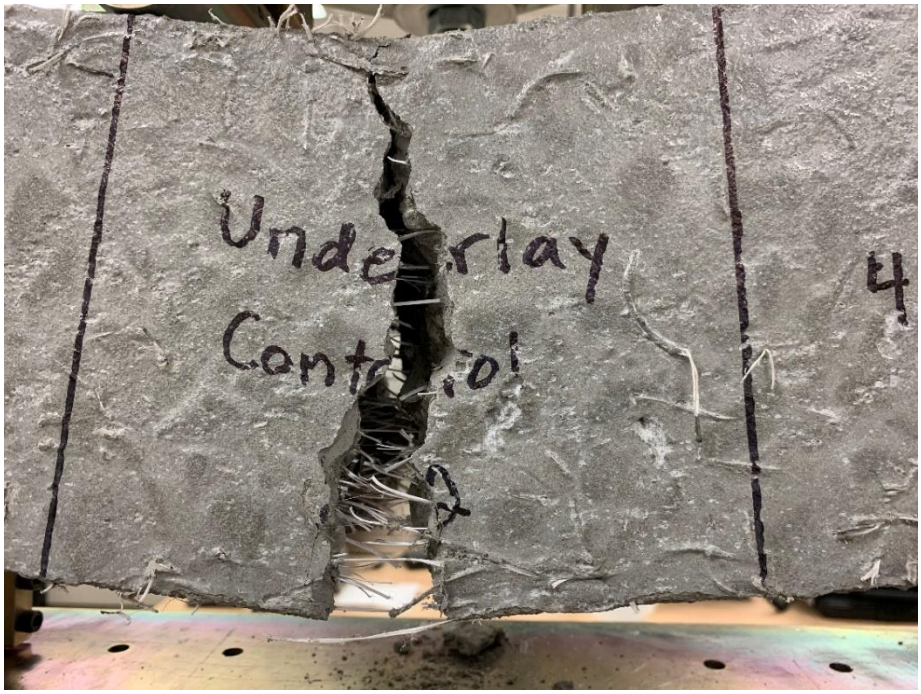

Figure 20. Fiber 2 FRC beam at end of test.

The load vs. deflection curves for the FRC beams with Fiber 3 are shown in Figure 21. These load vs. deflection curves are similar to the curves from Fiber 2. However, these curves seemed to show three peak loads, or an extra cycle of strain hardening, and strain softening compared to the other fibers. This may be a failure in the microfibers followed by a failure in the macro fibers. One beam shown, Beam 3, was an outlier and was excluded from all further calculations. This failed test was attributed to an error with the data acquisition software during testing. Since the behavior of the other two beams were in good agreement, a third beam wasn't considered necessary. As shown in Figure 21, the first peak occurred at a deflection of approximately 0.05 in., and the second peak occurs at a deflection of 0.15 to 0.20 in. These behaviors are consistent with Fiber 2. Both beams initially cracked within the middle third of their span at a nearly identical load of 8,000 pounds. One of the FRC beam breaks for Fiber 3 is shown in Figure 22.

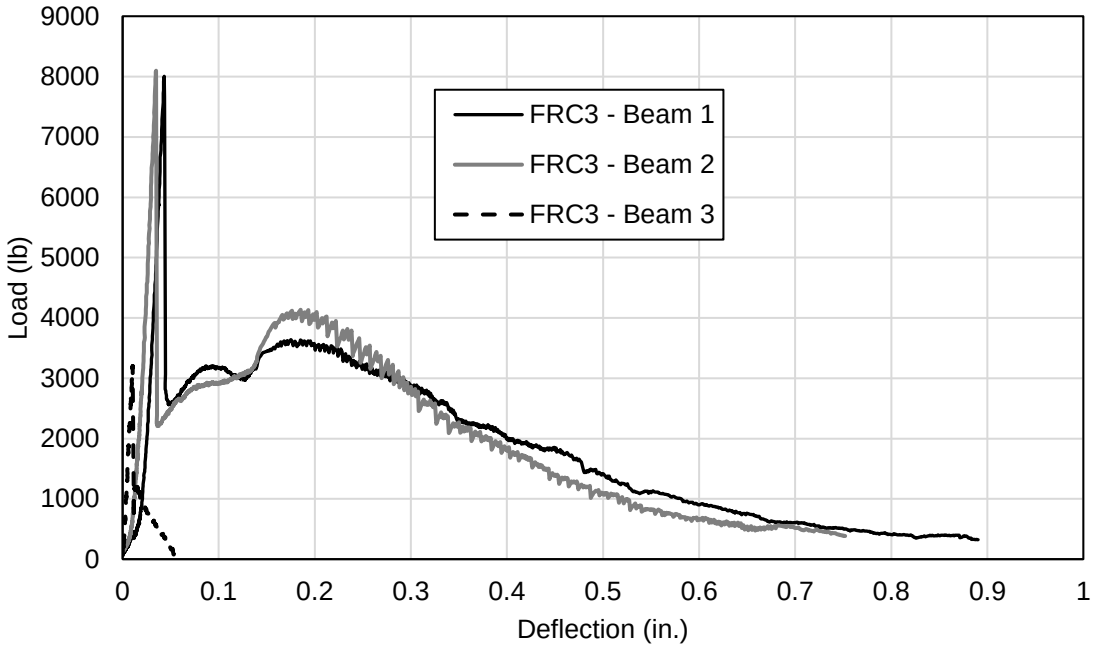

Figure 21. Load vs. deflection curves for Fiber 3 FRC beams.

Figure 22. Fiber 3 FRC beam at end of test.

The Fiber 4 FRC beam load vs. deflection curves are shown in Figure 23. Many similarities can be observed between the Fiber 3 and Fiber 4 curves. The Fiber 4 beams also initially cracked at a deflection of approximately 0.05 in., but strain hardening did not occur for as long as the other fiber types. Maximum strain hardening occurred at 0.1 in. All three FRC beams for Fiber 4 initially cracked within the middle third at a break load averaging 7,250 pounds for the beam set. A FRC beam at end of test for Fiber 4 is shown in Figure 24.

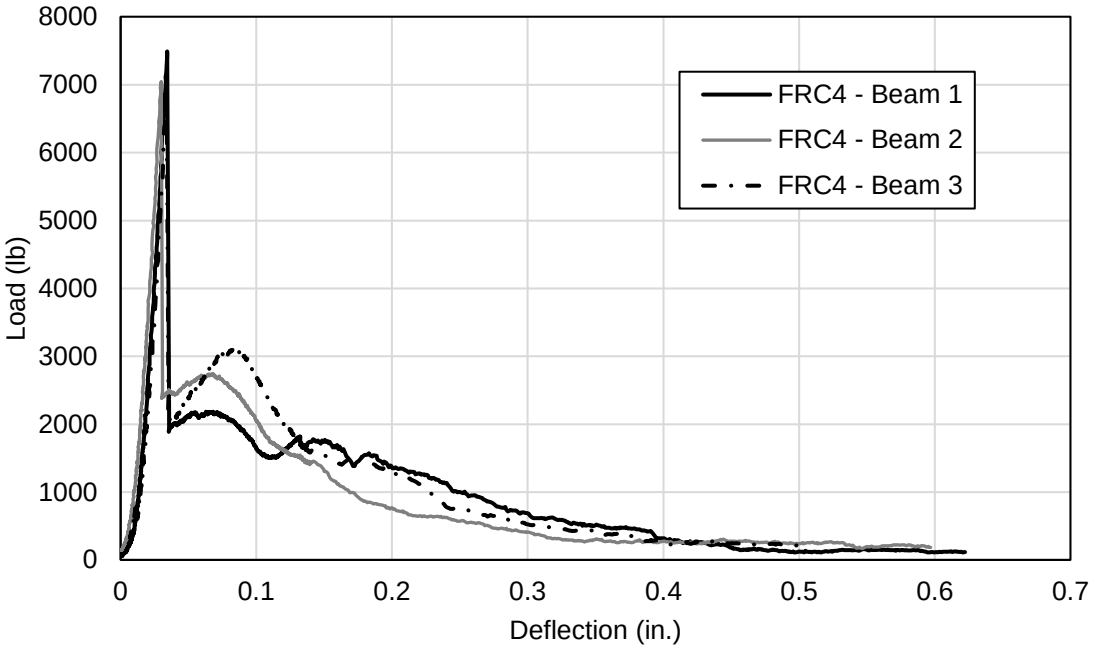

Figure 23. Load vs. deflection curves for Fiber 4 FRC beams.

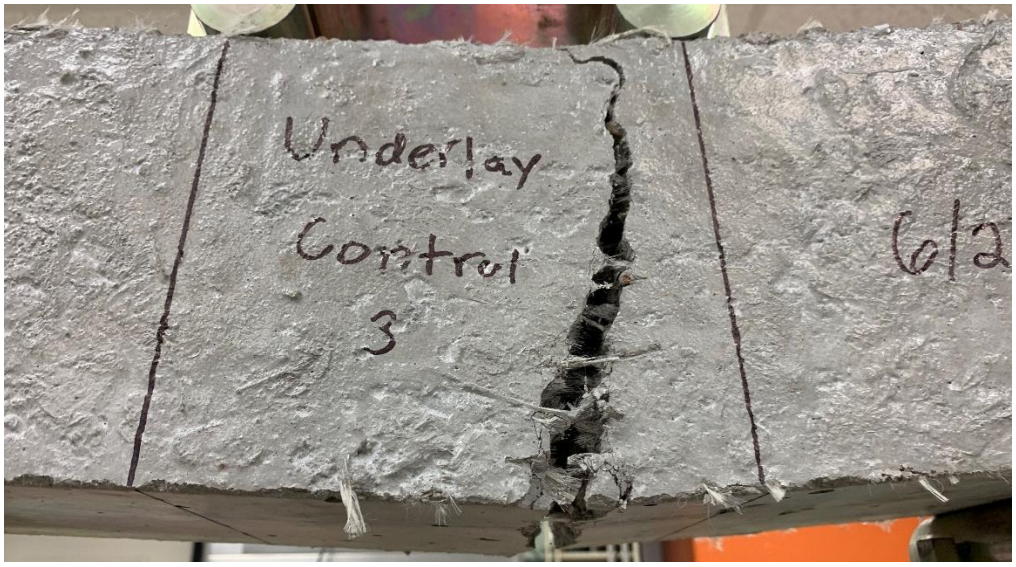

Figure 24. Fiber 4 FRC beam at end of test.

As stated previously, the load vs. deflection curves for beams containing fiber reinforcement showed a general trend of an initial peak at initial cracking, an incomplete loss of strength, and then strain hardening resulting in a gain of strength up to a percentage of its original strength. These points of interest were quantified for each

FRC beam tested. The first quantity compared between all these beams was the percentage of original strength retained after initial failure. This is shown in Figure 25. As shown in Figure 25, the FRC beams retained an average of 28% of their original strength after initial cracking. Fiber 1 retained the lowest percentage of the original strength after initial cracking while the other fiber types retained around 30% of their initial strength.

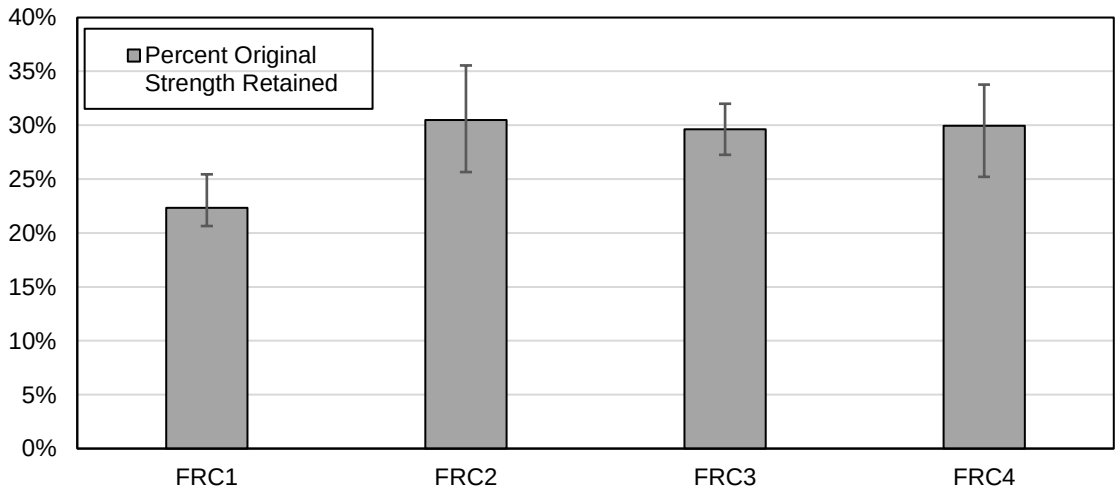

Figure 25. Percentage of original strength retained after initial cracking for all FRC beams.

The percentage of the original strength that the beams recovered during their strain hardening process was evaluated next. This is shown in Figure 26. Figure 26 also shows that all fiber types performed similarly in terms of the strength gain during strain hardening. On average, 43% of the cracking strength was regained during strain hardening across fiber types. Therefore, one can surmise that the addition of fiber reinforcement throughout the full depth of the section makes it possible for the section to carry more than 40% of its initial cracking load compared to PC which loses all strength after cracking.

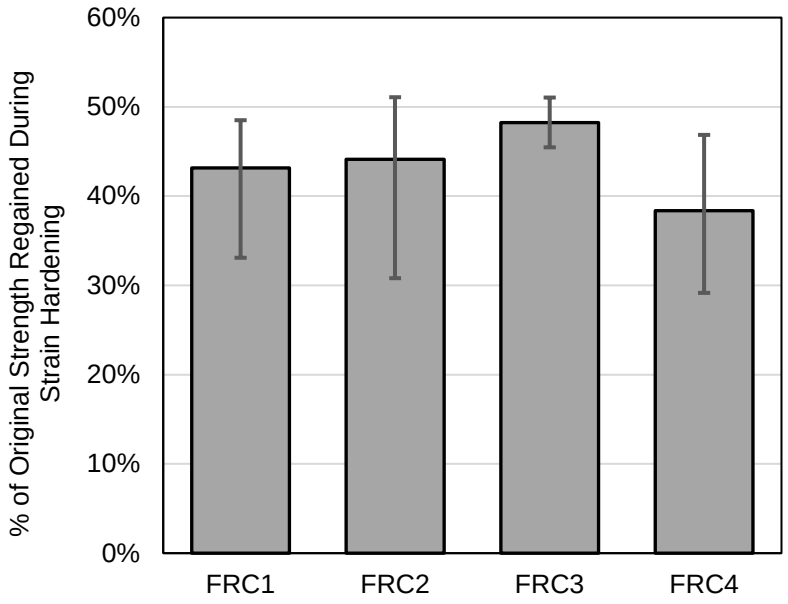

Figure 26. Percentage of original strength gained during strain hardening for all FRC beams.

4.4.3 Hybrid Beam Test Results

The hybrid PC-FRC beam failures were similar to the failures in the FRC specimens; they failed in a ductile manner due to having tensile reinforcement (fibers) in the tension zone (bottom section of the beam). A cross section view of this hybrid section and an illustration of a hybrid section at ultimate failure is shown in Figure 27. In the following figures, “H1N1” refers to hybrid beam 1 from Fiber 1 with no surface preparation, “H1D1” refers to hybrid beam 1 from Fiber 1 with the DELVO surface preparation method, and so on.

Figure 27. Example of hybrid cross section (left) and hybrid section at end of test (right).

Figure 28 shows the load vs. deflection curves for the hybrid beams containing Fiber 1. There were two beams made per surface preparation method and are grouped by line type and shading in the figure. These beams initially failed at a deflection of 0.03 to 0.05 in., and experienced strain hardening until a deflection of about 0.1 in. Most of these beams cracked within the middle third but beams H1T1 and H1D1 cracked on the middle third line, directly below one of the load application points. This was likely due to the beam geometry causing one of the load points to apply a slightly higher load than the other. This was mitigated during each beam break thereafter to try to minimize these effects. Even though this occasionally occurred throughout testing, it did not appear to significantly affect beam strengths. The first peak loads for the hybrid beams averaged to about 5,500 pounds. When observing the different surface preparation methods, they did not seem to affect the initial cracking load. For example, the tined beams had the highest and the lowest strengths in Figure 28. An example of a hybrid beam after testing was completed for Fiber 1 is shown in Figure 29.

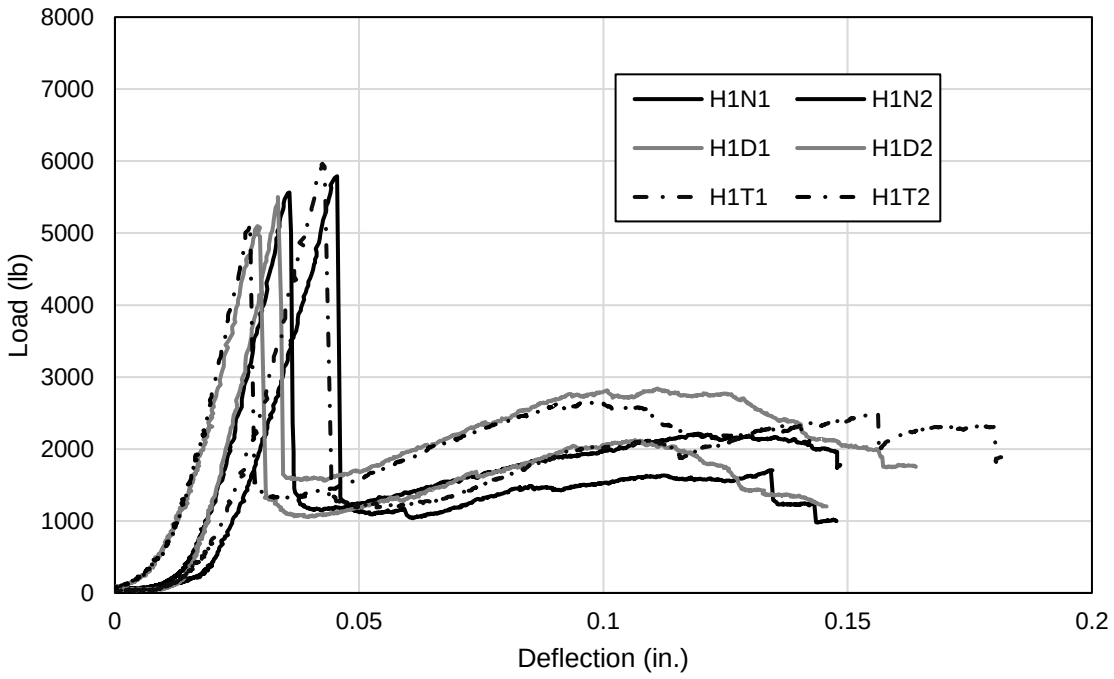

Figure 28. Load vs. deflection curves for Fiber 1 hybrid beams.

Figure 29. Fiber 1 hybrid beam at end of test.

The load vs. deflection curves for the hybrid beams with Fiber 2 are shown in Figure 30. Fiber 2 hybrid beams, unlike Fiber 1 hybrid beams, exhibited little to no strain hardening. The concrete initially cracked at a deflection of approximately 0.03 to 0.04 in., and did not gain strength like the others until a deflection of approximately 0.1 in. Most beams broke within the middle third, except for beams H1N1 and H1T2, which broke on the load point caused by the uneven loading discussed previously. All of the Fiber 2 hybrid beams initially cracked at an average break load of 5,900 pounds. The hybrid beams for Fiber 2 show the same results as Fiber 1 with respect to surface preparation; all cracking strengths were similar, and each surface preparation method is inconsistent in break strengths. The DELVO beams had almost identical strengths as the beams that were tined. There is no clear trend to say that one method was better than the other for this fiber type. An example of one of the hybrid beams at the end of testing is shown in Figure 31.

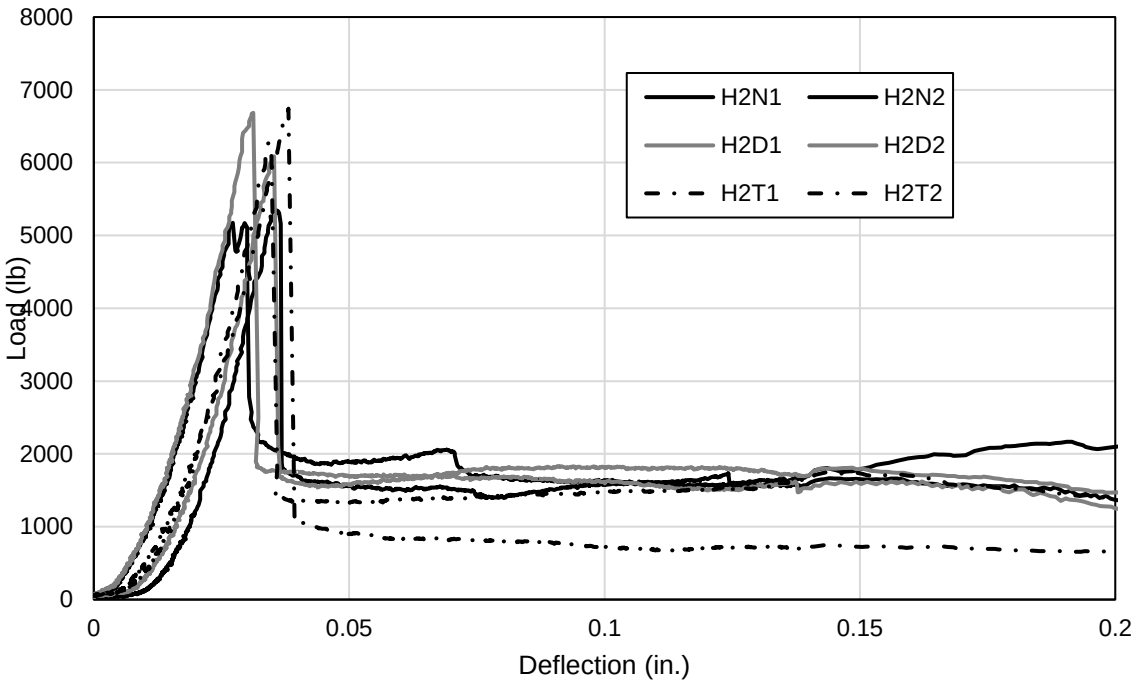

Figure 30. Load vs. deflection curves for Fiber 2 hybrid beams.

Figure 31. Fiber 2 hybrid beam at end of test.

The load vs. deflection curves for the Fiber 3 hybrid beams are shown in Figure 32. The hybrid beams for Fiber 3 lost less strength than the hybrid beams for Fiber 2, and thus, had more strain hardening. These beams initially failed at a deflection ranging from 0.02 to 0.05 in. and experienced strain hardening up until a deflection of about 0.1 in., similar to Fiber 1's hybrid specimens. All Fiber 3 hybrid beams cracked in the middle third, with only the beam H1N2 experiencing cracking under the load point. The beams experienced a first peak load of 5,500 pounds for the set. Surface preparation methods did not have a clear effect on this fiber type. One of the beam breaks from Fiber 3 is shown in Figure 33.

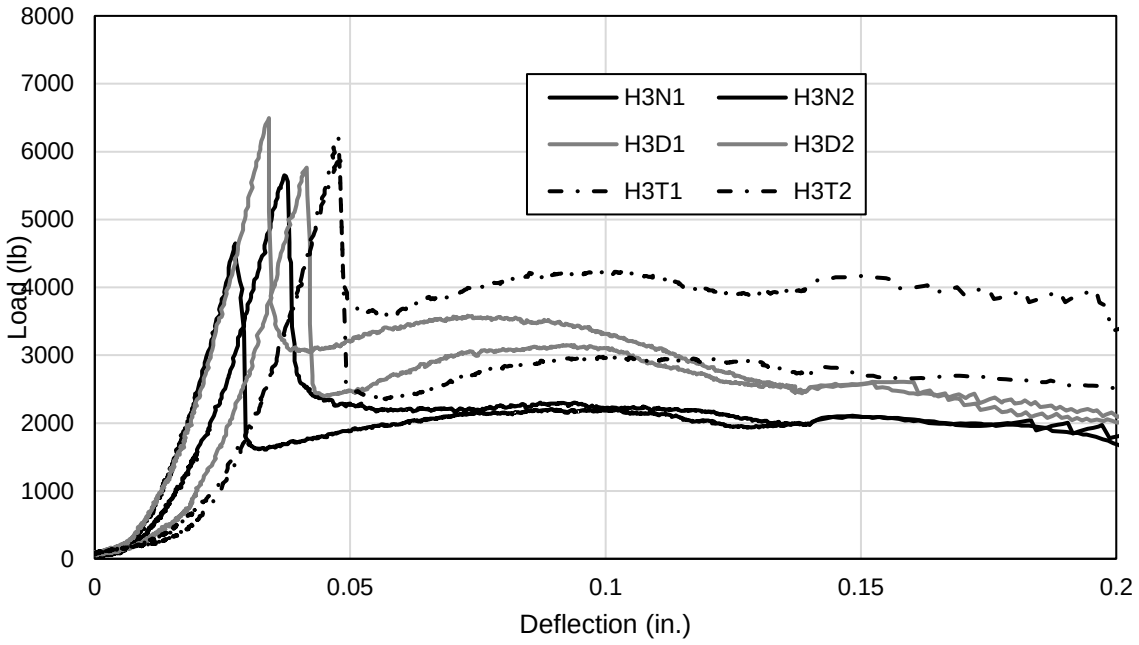

Figure 32. Load vs. deflection curves for Fiber 3 hybrid beams.

Figure 33. Fiber 3 hybrid beam at end of test.

The load vs. deflection curves for Fiber 4 are shown in Figure 34, and are similar to those of Fiber 1. Similarities continue through the second peak, indicating a clear region of strain hardening. The Fiber 4 hybrid beams failed at deflections ranging from 0.03 to 0.04 in. and experienced strain hardening until a deflection of around 0.08 in. All beams in this set initially cracked within the middle third of the span at an average break load of 7,250 pounds for the set. The DELVO method and the tines method resulted in the highest strengths for this fiber type. An illustration of one of the hybrid beam breaks for the Fiber 4 set is shown in Figure 35.

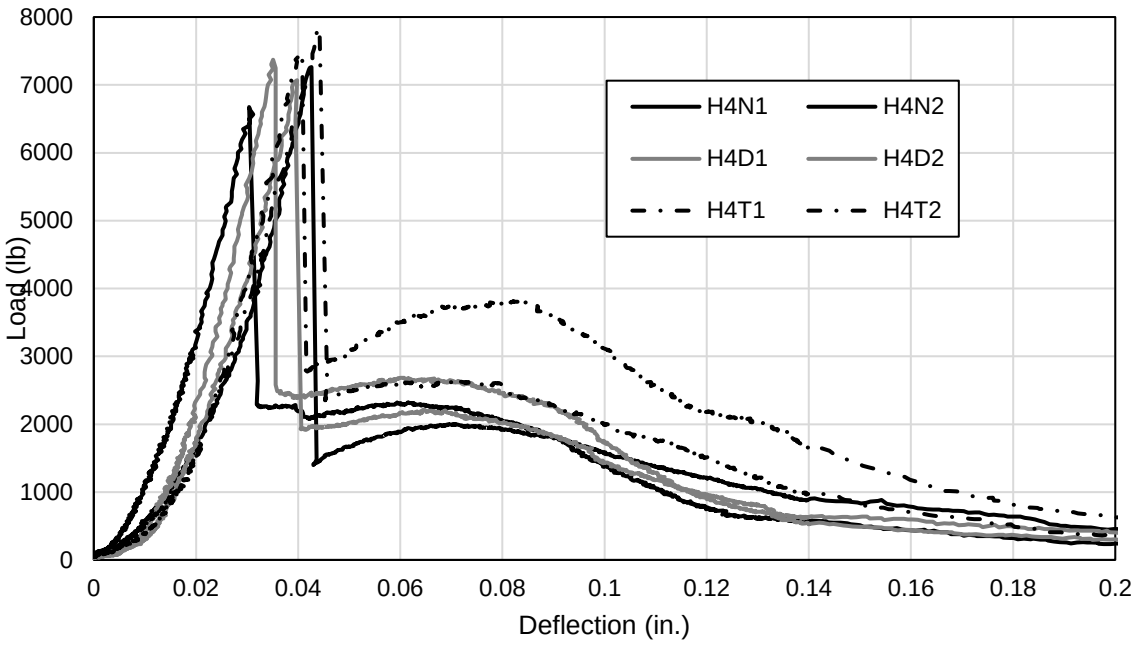

Figure 34. Load vs. deflection curves for Fiber 4 hybrid beams.

Figure 35. Fiber 4 hybrid beam at end of test.

To align with the previous section, the points of interest on the load vs. deflection curves were also quantified for the hybrid beams. The percentages of original strength that were retained after initial cracking were examined for the hybrid beams, as well as the percentages of original strength that were gained during the strain hardening process, if there was one. The retained strengths after failure are shown in Figure 36. Figure 36 shows an average of the beams with each surface preparation method within each fiber type. For example, HN for Fiber 1 is the average of the two beams from Fiber 1 that had no surface preparation applied to them. This figure shows that all types of hybrid beams for Fiber 3 had the highest percentage of their original strength retained after initial cracking, suggesting that a blend of micro and macro fiber types (described in Section 3.1.1) reduces the flexural strength loss after initial cracking. The Fiber 3 hybrid beams had an average strength retained of 43% compared to 29% for the Fiber 3 FRC beams. The hybrid beams for the other fiber types were either less than or around the same percentage as their respective FRC beams.

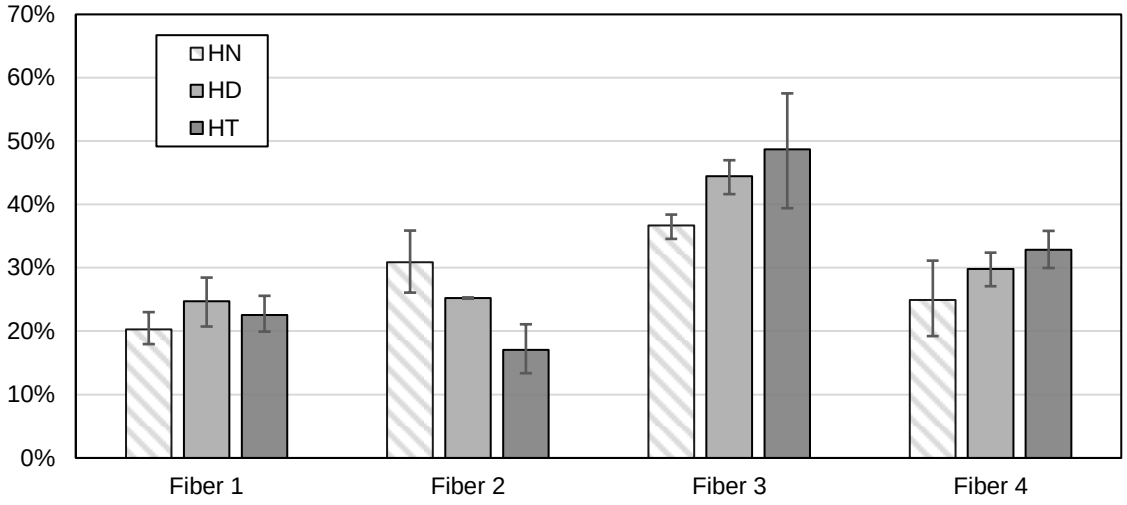

Figure 36. Percentage of original strength retained after initial cracking for all hybrid beams.

The percent of the initial pre-cracking strength regained during strain hardening is shown in Figure 37. For the most part, this figure shows the same trend as Figure 36. The beams containing Fiber 3, specifically the DELVO and tined beams provided the highest strength gain during strain hardening. Thus, the hypothesis formed in the previous section holds true. All fibers help the cracked concrete retain its strength and enhance the concrete's strength gain after initial failure, but Fiber 3 was more effective than the other fibers. The Fiber 3 hybrid beams gained 53% of their original strength compared to 48% with the Fiber 3 FRC beams. The hybrid beams for the other fiber types were either lower or around the same strength gain as their respective FRC beams. It is also important to notice that in both figures, and excluding Fiber 2, the DELVO and tined beams regained higher percentages of their original strength than the beams with no surface preparation. This distinction is significant and will be expanded upon in further sections.

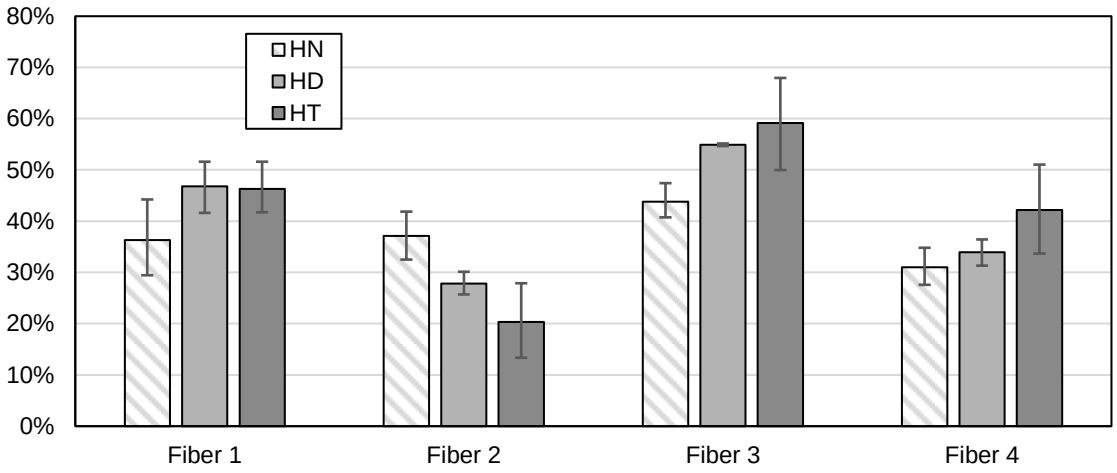

Figure 37. Percentage of original strength gained during strain hardening for all hybrid beams.

5. Discussion

5.1 MOR

The first criterion that was evaluated from the load vs. deflection curves presented previously was flexural strength, or modulus of rupture (MOR). The MOR was calculated in this research by using the equation outlined in ASTM C1609 [35] and these values were then compared to values from the MOR equation outlined in ACI 318-14 [37]. The experimental MOR per ASTM C1609 was calculated using Equation 1:

Equation 1

$$f = \frac{PL}{bd^2}$$

Where:

f = MOR (psi)

P = first peak load (lb.)

L = span length (in.)

b = average width of beam at fracture location (in.)

d = average depth of beam at fracture location (in.) [35]

The first peak load was recorded during testing, the span length for the loading setup used was 18 in. from support to support, and the widths and depths of each member were measured with a digital caliper after testing was completed. The MOR values calculated with this method were then compared to the MOR equation found in ACI 318-14 as Equation 19.2.3.1 but defined as Equation 2 here:

Equation 2

$$f_r = 7.5\lambda\sqrt{f'c}$$

Where:

f_r was the predicted MOR for concrete

λ was a lightweight factor for concrete, taken as 1.0 here (normal weight concrete)

$f'c$ was the concrete compressive strength at 28 days taken from Table 6 [37]

For the hybrid sections, it was decided to use the $f'c$ value for the bottom layer of concrete because this is where the cracking would originate (at the extreme tension fiber of the beams). All final MOR values for each beam type are shown in Table 8. In Table 8, each beam type was averaged across fiber types. When comparing the ACI MOR and the experimental MOR, the experimental values were predicted closely. All beam types, except for the hybrid beams without surface preparation (HN), fell within 10% of the flexural strength value predicted by Equation 2. As a whole, it cannot be said that either the addition of fibers or the utilization of different surface preparation methods impacted the flexural strength for better or for worse.

Table 8. Averaged MOR values for all beam types.

Beam	Experimental MOR (psi)	ACI MOR (psi)	Experimental / ACI MOR Ratio	Experimental MOR Standard Deviation (psi)
FRC	565	560	1.01	52.7
PC	535	548	0.98	81.0
HN	480	560	0.86	65.5
HD	520	560	0.93	59.1
HT	540	560	0.96	72.2

Note: FRC = Fiber Reinforced Concrete, PC = Plain Concrete, HN = Hybrid None, HD = Hybrid DELVO, HT = Hybrid Tines.

Figure 38 shows this similarity of all flexural strengths between fiber types and between beam types. The flexural strengths for each beam type were normalized according to the square root of their respective concrete compressive strengths, $f'c^{1/2}$, to reduce any unnecessary variation. The hybrid beams were normalized according to the f'c of the fiber layer in the bottom of the concrete because this is the layer that would experience flexural stresses. For example, All FRC beams for Fiber 3 and all hybrid beams for Fiber 3 were normalized according to the 28-day strengths (f'c) for FC3 in Table 6. As stated previously, this figure shows the similarity between the experimental MOR values and the MOR values calculated using ACI. When the cracking strengths of the beams were normalized by compressive strength, there appeared to be little difference between fiber types or beam designs.

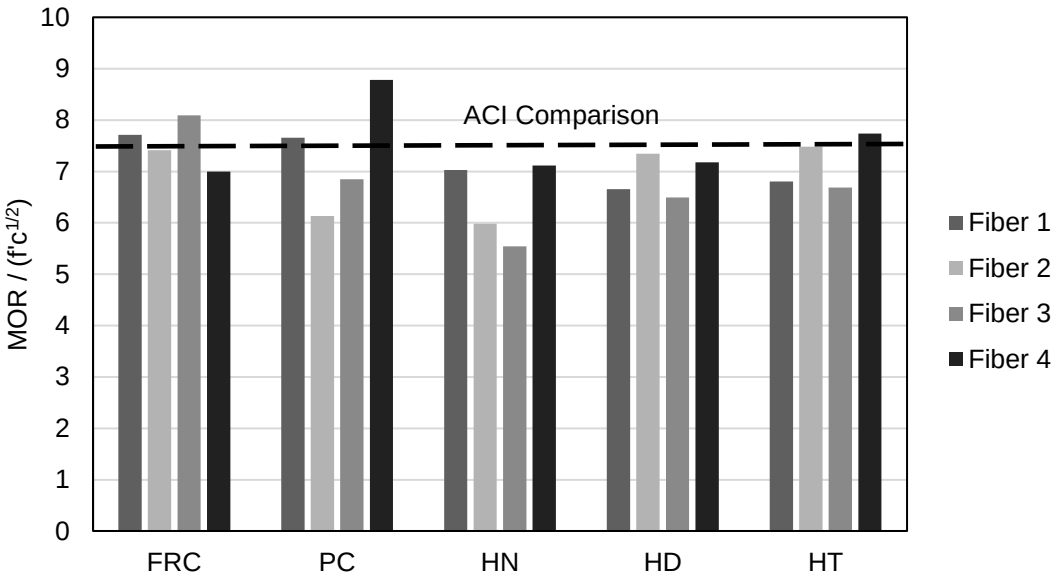

Figure 38. Normalized MOR values for all beam specimens.

With each batch of PC made as the top layer of the hybrid beams, companion PC beams were cast as control beams. One can see in Figure 38, that the PC beams made during the 4th batch had much higher flexural strengths than the others. As stated in Section 4.4.1, the reason for this spike in flexural strengths is unknown since no variables were changed between these batches of PC. The mix designs were the same, the same molds were used, the compressive strengths were similar, and the air content was not low compared to the others. The average flexural strength for all PC beams was around 535 psi.

The flexural strengths for the FRC beams can also be evaluated separately in Figure 38. One can see that Fiber 3 had the highest flexural strengths between all four fiber types, although not by much. Therefore, when evaluating the fully fiber reinforced beams, one cannot say that the addition of one fiber type greatly increased the MOR when compared to the others. The modulus of rupture values for the hybrid beams were

also all similar. Fiber 4 consistently had the highest cracking strength for each hybrid beam type.

5.2 Beam Toughness Results

The second and more important property of these beams was their toughness. The MOR only evaluates the strength when a flexural crack appears. Toughness is a better representation of load carrying capacity after cracking and the resistance to deformation of the specimens. For a pavement application, the toughness should provide a measure of how well the concrete maintains its load-carrying capabilities after cracking. Typically, the more ductile the material, the higher the toughness [23]. During this research, the toughness was calculated by computing the area under the load vs. deflection curves for each beam as outlined in ASTM C1018 [38]. It was determined that two separate toughness areas were of interest: the toughness up until the first crack formed (first peak), sometimes referred to as the initial toughness in this paper, and the toughness between the first crack (first peak) and the second peak in the load vs. deflection curves, occasionally referred to as the secondary toughness in this paper. As discussed previously, the curves for the beams with fiber reinforcement showed these typical points of interest. An example of how toughness was calculated is shown in Figure 39. The initial toughness value, toughness to the first peak, relates to the beam's toughness up to the deflection when it initially cracked. As discussed previously, once the beam cracked, it lost a percentage of its strength, but gradually regained some strength over time through strain hardening. This ability to regain strength during strain hardening after initial failure was captured with the secondary toughness value. Therefore, all beams could be compared in their ability to resist initial cracking but could

also be compared in their ability to regain strength after initial failure. Toughness values after the second peak were not considered because each beam test was ended at variable deflections based on how long it took them to lose all their load carrying capacity. It was determined that the toughness up to the second peak load was the more relevant metric. The toughness values up to the first peak for all beams are shown in Figure 40.

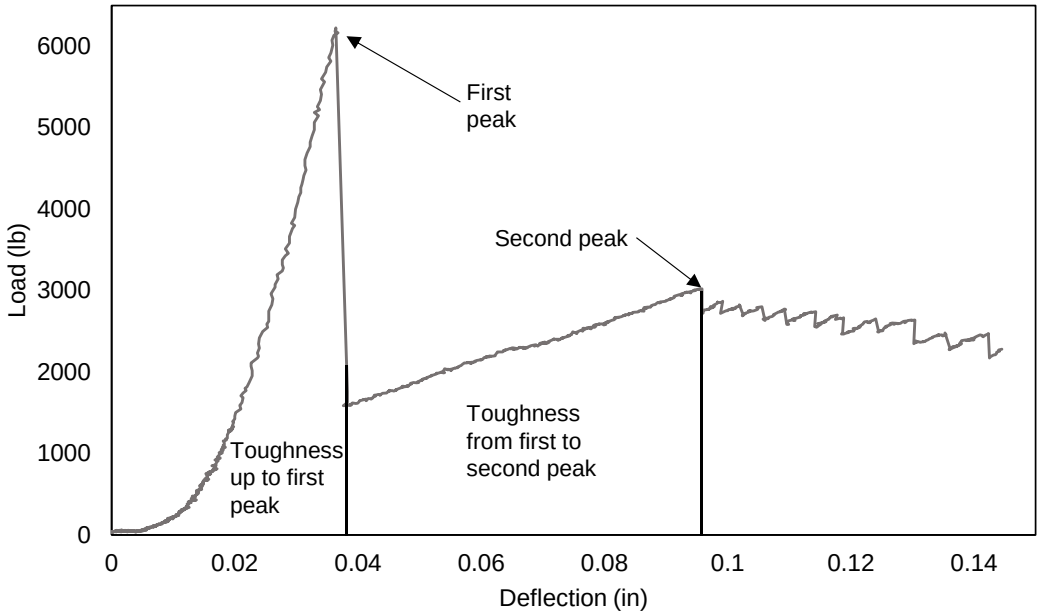

Figure 39. Points of interest on load vs. deflection curve used to evaluate toughness.

Figure 40 shows that most toughness values up to the first crack are similar. This makes sense since all the MOR values shown previously (Figure 38) were similar. However, the Fiber 4 initial toughness values stand out. The initial toughness values for the PC beams averaged around 120 lb-in. The initial toughness values for the FRC

beams are similar to the initial toughness values for the PC beams shown in Figure 40. These initial toughness values averaged around 140 lb-in.

The initial toughness values for the hybrid beams averaged around 145 lb-in. However, Fiber 4 had a consistently higher toughness than the other fiber types. When Fiber 4 is excluded, the average initial toughness value for the hybrid beams was around 100 psi. Fiber 4 produced significantly higher initial toughness values.

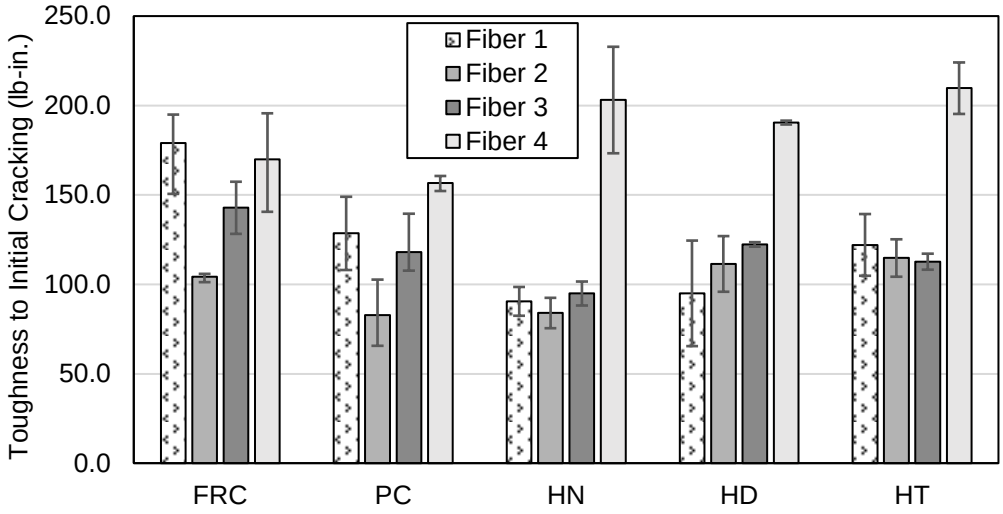

Figure 40. Comparison of toughness to first peak for all beams.

The secondary toughness values in between the first and second peak for the beams with fibers are shown in Figure 41. There was a clear trend in the toughness values after the first crack between beam types. As stated previously, the PC had no toughness (or strength) after the first cracking occurred and therefore is not included in this figure. The toughness values after cracking were the highest for the FRC beams. The hybrid sections have some toughness after cracking, but not as much as the fully reinforced concrete beams. This is because there was more fiber bridging the flexural crack to enhance ductility throughout the section in the beams with fiber in the full depth

instead of just in the tension zone. The hybrid beam toughness after initial cracking can also be reported as a percentage of the toughness of the FRC beams. The hybrid beams with Fiber 1 had approximately 83% the toughness of the FRC beams with Fiber 1, whereas the hybrid beams for Fiber 2 were 40% the toughness of their respective FRC beams, the Fiber 3 hybrid beams were 36%, and the Fiber 4 hybrid beams were 80% as tough after cracking when compared to their respective FRC beams.

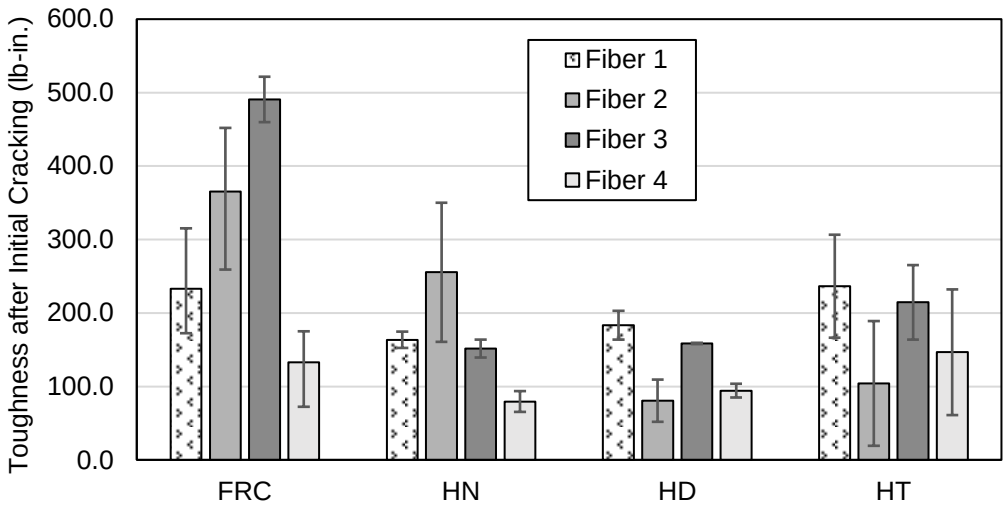

Figure 41. Comparison of toughness from first to second peak for all fiber beam types.

The average toughness for the FRC beams from the first peak load to the second peak load was around 305 lb-in., which was more than twice their initial toughness values. This is because they carried load and continued to deflect for a long time after initial cracking. Fiber 4 had the lowest toughness after initial cracking, whereas Fiber 3 had the highest toughness after initial cracking. The main reason that Fiber 3 had the highest toughness after initial cracking could be due to that specific fiber type being a blend of micro- and macro-fibers types.

The secondary toughness values for the hybrid beams averaged at roughly 170 lb-in. The toughness values after initial cracking up to the second peak showed trends between fiber types, and surface preparation methods. The toughness for Fiber 4 decreased sharply once initial cracking occurred as discussed earlier, where the other fiber types retained their toughness and ductility and even increased in toughness in most cases after initial cracking. One can also notice that all the hybrid beams have very similar toughness values before initial cracking (130 lb-in. average from Figure 40), and after initial cracking up to the first peak (160 lb-in. average from Figure 41).

The initial and secondary toughness values were summed together to form the total toughness which is shown in Figure 42. The total toughness values shown in Figure 42 show a similar trend as Figure 41 which summarized the toughness after initial cracking up to the second peak load. The FRC beams have the highest total toughness values, followed by the hybrid sections, and then lastly the PC beams with the lowest. Each surface preparation method and its effect on strength and toughness will be discussed in detail in Section 5.3. The addition of a bottom fiber reinforced layer roughly doubled the toughness compared to PC.

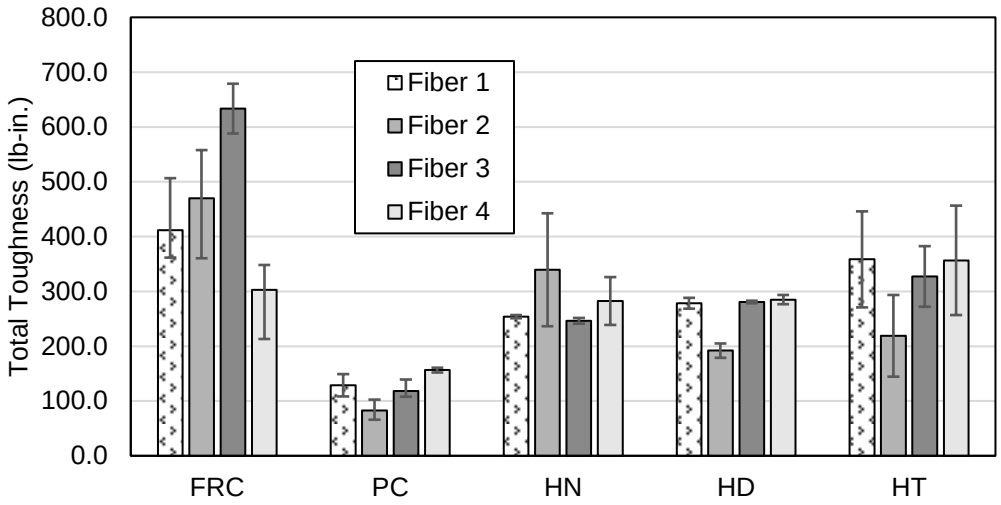

Figure 42. Comparison of total toughness for all beams.

As already discussed, when the PC beams failed, they had no strength and no toughness after. Therefore, the toughness shown for the PC beams is only the toughness up to the first crack and is also the total toughness. The total toughness figure (Figure 41) appears identical to the secondary toughness figure (Figure 42) for the FRC beams and hybrid beams. This would indicate that the initial toughness values that were added to the secondary toughness values did not have impact on the final toughness values.

When evaluating the total toughness values for all the hybrid beams, there is a similarity between fiber types. Another way that these total toughness values for the hybrid beams can be presented is as a percent of the total toughness of the fully FRC beams, as shown in Figure 43.

Figure 43 shows each hybrid toughness as a percentage of their respective FRC toughness values. For example, Hybrid 1 None beams had roughly 60% of the total toughness of the FRC beams of Fiber 1. Therefore, in this case, reinforcing roughly half

the depth of the beam as opposed to the full depth, results in 60% of the toughness of a section with fiber reinforcement fully throughout the depth. However, the hybrid beams for Fiber 4 show total toughness values ranging from 90% to 120% of their fully fiber reinforced companion beams. This would suggest that with some fiber types a hybrid section may provide similar toughness benefits to a full-fiber reinforced section while providing the added benefit of easier surface finishing. Fiber 4 unraveled and became very stringy after the mixing process. It is hypothesized that this is the cause for the improved post-cracking toughness in the hybrid beams. An illustration of this phenomenon is shown in Figure 44.

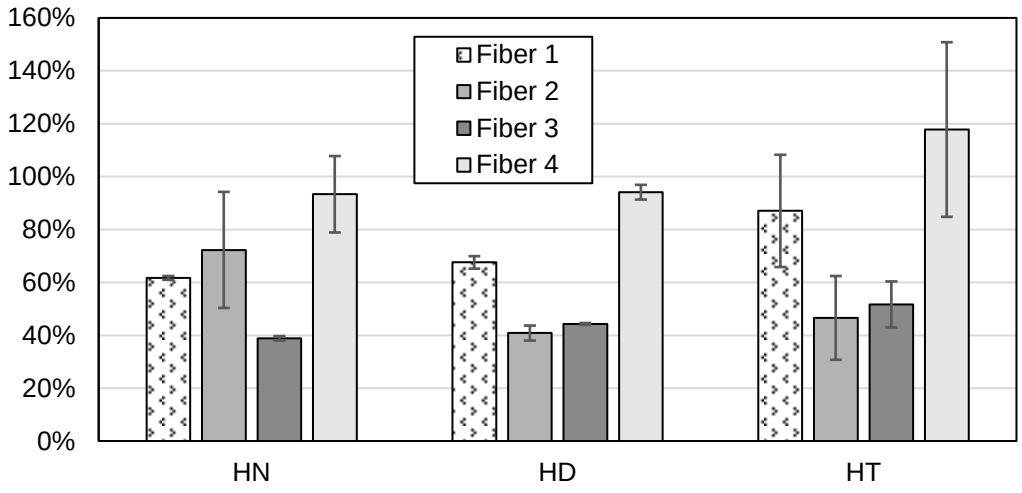

Figure 43. Total toughness of hybrid beams as a percent of their respective FRC beams.

Figure 44. Fiber 4 after mixing.

Previously in Section 2.1, it was discussed that it was difficult to keep the layers of the hybrid concrete specimen's constant, resulting in varying layer depth in the FRC concrete layer. Thus, all layer depths were recorded for reference. Throughout the study, it was decided to examine the effects of these varying layer depths on the effects of the total toughness of the beams. There was no clear trend when evaluating the effects of the FRC layer depth in relation to the total toughness of the specimen. This comparison is shown in Figure 45. There did not appear to be a clear relationship between fiber layer depth and total toughness of the hybrid specimens for the range of fiber layer depths observed.

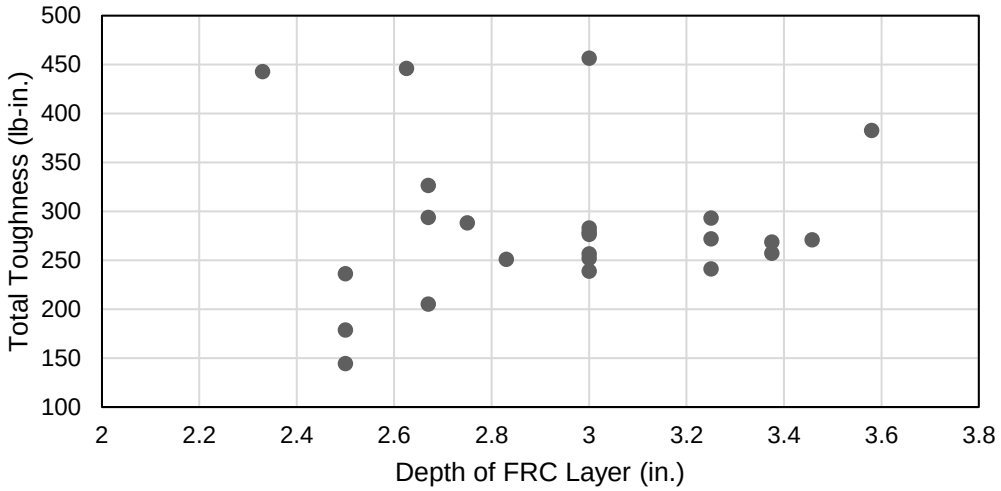

Figure 45. The effect of the depth of the FRC Layer on the total toughness of the hybrid beams.

5.3 Comparison of Surface Preparation Methods

To organize the presentation of data, it was decided to have a separate section to compare the effectiveness of the surface preparation methods. This section will reference figures and topics discussed from previous sections within the results. The surface preparation methods will be compared regarding their effect on strengths and their effects on toughness of the beam specimens.

5.3.1 MOR Comparison

When evaluating Table 8 in Section 4.5, it showed that all surface preparation methods provided similar strengths to those predicted by Equation 2. Therefore, it cannot be said that one surface preparation method increased or decreased the flexural strengths of the hybrid beams. This trend can also be observed in Figure 38 in Section 5.1. The same conclusions can be drawn from all the hybrid beam load vs. deflection curves shown in Section 4.4.3. Therefore, it can be concluded that the surface

preparation method did not have a large effect on the flexural strength of the concrete specimens.

5.3.2 Toughness Comparison

When examining all the toughness figures in Section 5.2, a summary table was created to show the actual values for each hybrid beam type. This summary table is shown in Table 9.

Table 9. Direct comparison of toughness values for each hybrid beam type.

Beam Type	Toughness to Initial Cracking (lb-in.)	Toughness After Initial Cracking (lb-in.)	Total Toughness (lb-in.)
H1N	90	165	255
H1D	95	185	280
H1T	120	240	360
H2N	85	255	340
H2D	110	80	190
H2T	115	105	220
H3N	95	150	245
H3D	120	160	280
H3T	110	215	325
H4N	200	80	280
H4D	190	95	285
H4T	210	145	355

When taking a closer look at the values in the table, in the majority of cases the hybrid beam with the tines surface preparation (H1T, H2T, etc.) provided the highest toughness values before and after initial cracking occurred. Before cracking, the averaged values were as follows: 140 lb-in. for Tines, 130 lb-in. for DELVO, and 120 lb-in. for the beams with no surface preparation. The specimens with no surface preparation and the DELVO specimens produce inconsistent results. Some specimens experienced higher toughness before cracking in the DELVO beams while others

experienced the highest toughness before cracking in the specimens with no surface preparation. The toughness values after cracking were 180 lb-in. for Tines, 160 lb-in. for the specimens with no surface preparation, and 130 lb-in. for the DELVO specimens. The total toughness values for the surface preparation methods were 315 lb-in. for Tines, 280 lb-in. for “None”, and 260 lb-in. for DELVO. Therefore, the Tines provided the best overall results, followed by the beam specimens with no surface preparation, and lastly by the DELVO specimens.

5.3.3 Visual Observations of Bond Failures

During testing, it was observed that the specimens without surface preparation experienced a bonding failure between the two layers of concrete across 3 of the 4 fiber types. Some bond failures were more severe than others. The shearing stresses at the middle of the section caused the top layer to debond from the bottom layer. This occurred when the cracks traveled along the boundary interface. This debonding failure happened after the second peak in the load vs. deflection curves and continually got worse as the beam was loaded. This debonding failure could be a concern when exposed to long-term flexural loading, but since these cracks occurred after the second peak in the load versus deflection curve, all methods appeared to provide sufficient bonding. An illustration of this debonding failure at the end of testing of this is shown in Figure 46.

Figure 46. Worst case bond failure for hybrid beam with no surface preparation between layers at end of test.

Flexural cracking started at the bottom in the middle third of the beam, indicating a proper failure. However, as the loading continued, the cracks traveled up to the boundary interface, and spread out horizontally. These cracks formed horizontally until they reached the point load locations, and then they went straight up to the load point. Therefore, after observing this phenomenon, it is highly recommended to use a surface preparation method (preferably one that cuts grooves like tines) when casting a hybrid section and not to leave the boundary interface untreated.

6. Conclusions

When summarizing all of the results presented previously, many conclusions can be drawn in relation to beam types, fiber types, and surface preparation methods. The conclusions made regarding to the beam types were the following:

- When considering the MOR for the beams tested in this study, the inclusion of fibers throughout the depth or in the tension region did not increase the flexural strength.
- The FRC beams had more secondary toughness than initial toughness resulting in increased total ductility.
- The hybrid beams have similar toughness values before and after cracking
- Adding a layer of fiber reinforcement, as done in the hybrid beams, doubled the total toughness when compared to PC beams. This hybrid approach would improve pavement performance while ensuring a top layer that is easy to finish.

The conclusions made regarding the different fiber types were as follows:

- Fiber type, like beam type, did not affect the MOR of the specimens
- The addition of fiber reinforcement throughout the full depth of the section (FRC beams) resulted in a strength gain after initial cracking of roughly half of its original strength before cracking
- Fiber 3, a blend of fiber types, resulted in the highest percent of this strength gain. Therefore, a blend of fibers reduces the flexural strength loss after initial cracking forms

- Fiber 4 provided similar toughness benefits in a hybrid section to a FRC section while providing the added benefit of easier surface finishing.

The conclusions made regarding the different surface preparations in the hybrid beam sections and the hybrid slant shear cylinders were:

- Surface preparation method did not have an effect on the flexural strength
- Beams with the tines method resulted in the highest total toughness (315 lb-in.), followed by the beams without any surface preparation (280 lb-in.), and the beams yielding the lowest total toughness were the DELVO beams (260 lb-in.)
- During testing, it was observed that the hybrid beams without surface preparation experienced a bonding failure after significant deformation.
- The slant-shear specimens with the DELVO surface preparation method experienced failure along the interface, which resulted in lower strengths compared to the other surface preparation methods

6.1 Future Work

Many things could be evaluated in the future regarding a hybrid section of PC and FRC for pavement applications. The following should be examined in future work: evaluating more surface preparation methods, the performance of fiber types other than synthetic fibers, various fiber dosages, varying FRC layer depths, and various flexural specimen sizes (larger or smaller beams might yield different results). The results of this study were relevant only to a low dosage of synthetic fibers in small flexural specimens with only three different surface preparation methods. Varying any of these variables could wildly change the performance of a hybrid PC and FRC pavement section.

References

[1] A. A. Ghadban, N. I. Wehbe, and M. Underberg, “Fiber Reinforced Concrete For Structure Components”, *Mountain Plains Consortium (MPC),* 2017.

[2] F. F. Wafa, “Properties and Applications of Fiber Reinforced Concrete”, *Journal of King Abdulaziz University: Engineering Science*, vol. 2, pp. 49-63, 1990.

[3] D. H. Chen and M. Won, “Field Investigations of Cracking on Concrete Pavements”, *Journal of Performance of Constructed Facilities*, ASCE, 2007.

[4] Z. I. Raja and M. B. Snyder, “Factors Affecting Deterioration of Transverse Cracks in Jointed Reinforced Concrete Pavements”, *Transportation Research Record 1307*, 1991.

[5] R. S. *et al.*, “Brief History and Background of PCC Pavements,” *Composite Pavement Systems*, vol. B, 2013.

[6] American Concrete Pavement Association (ACPA), “Concrete Pavement Basics”, http://www.acpa.org/StreetPave/Concrete%20Pavement%20Basics.pdf.

[7] Portland Cement Association (PCA), “Concrete Pavement,” *2019*. https://www.cement.org/cement-concrete/products/concrete-pavement (accessed Oct. 21, 2021).

[8] R. F. Zollo, “Fiber-reinforced Concrete: an Overview after 30 Years of Development”, *Cement and Concrete Composites,* 1997.

[9] Fiber Reinforced Concrete Association (FRCA), “FAQ’s - Frequently Asked Questions,” Murfreesboro, TN, 2020.

[10] R. Barborak, “Texas Department of Transportation -Fiber Reinforced Concrete (FRC) - DMS 4550 Tip Sheet,” 2011.

[11] D. Ghosh, A. Abd-Elssamd, Z. J. Ma, and D. Hun, “Development of High-Early-Strength Fiber-Reinforced Self-Compacting Concrete,” *Construction and Building Materials*, vol. 266, Jan. 2021, DOI: 10.1016/j.conbuildmat.2020.121051.

[12] H. Wang, A. Belarbi, and B. Huanzi Wang, “Flexural Behavior of Fiber-Reinforced-Concrete Beams Reinforced with FRP Rebars.”

[13] L. Xu, L. Huang, Y. Chi, and G. Mei, “Tensile Behavior of Steel-Polypropylene Hybrid Fiber-Reinforced Concrete,” *ACI Materials Journal*, vol. 113, no. 2, pp. 219–229, Mar. 2016, DOI: 10.14359/51688641.

[14] M. Sarigaphuti, S. P. Shah, and K. D. Vinson, “Shrinkage Cracking and Durability Characteristics of Cellulose Fiber Reinforced Concrete,” *ACI Materials Journal*, 1993.

[15] M. Dopko, M. Najimi, B. Shafei, X. Wang, P. Taylor, and B. Phares, “Strength and Crack Resistance of Carbon Microfiber Reinforced Concrete,” *ACI Materials Journal*, vol. 117, no. 2, pp. 11–23, Apr. 2020, DOI: 10.14359/51720297.

[16] A. Macanovskis, A. Lukasenoks, A. Krasnikovs, R. Stonys, and V. Lusis, “Composite Fibers in Concretes with Various Strengths,” *ACI Materials Journal*, vol. 115, no. 5, pp. 647–652, Sep. 2018, DOI: 10.14359/51702343.

[17] N. Suksawang and A. Mirmiran, “Use of Fiber Reinforced Concrete for Concrete Pavement Slab Replacement,” 2014.

[18] M. Barman, S. Roy, A. Tiwari, and T. Burnham, “Performance Benefits of Fiber Reinforced Thin Concrete Pavement and Overlays,” *National Road Research Alliance*, 2021.

[19] U.S. Department of Transportation - Federal Highway Administration, “Highway Performance Monitoring System - Field Manual,” 2016. https://www.fhwa.dot.gov/policyinformation/hpms/fieldmanual/hpms_field_manual_dec2016.pdf (accessed Nov. 10, 2021).

[20] A. Nobili, L. Lanzoni, and A. M. Tarantino, “Experimental Investigation and Monitoring of a Polypropylene-based Fiber Reinforced Concrete Road Pavement,” *Construction and Building Materials*, 2013.

[21] Y. Chen, G. Cen, and Y. Cui, “Comparative Study on the Effect of Synthetic Fiber on the Preparation and Durability of Airport Pavement Concrete,” *Construction and Building Materials*, 2018.

[22] S. Plückelmann and R. Breitenbücher, “Experimental investigation of hybrid concrete elements with varying fiber reinforcement under concentrated load,” in *American Concrete Institute, ACI Special Publication*, Nov. 2020, vol. SP-343, pp. 422–431. DOI: 10.35789/fib.BULL.0095.Ch43.

[23] C. Gorse, D. Johnston, and M. Pritchard, *A Dictionary of Construction, Surveying and Civil Engineering*. Oxford University Press, 2020. DOI: 10.1093/acref/9780198832485.001.0001.

[24] Durable Products Group LLC, “SafeTcrete IMPACT Maximum Performance Fiber.” https://www.duratechnologies.com/safetcrete-impact/ (accessed Jul. 01, 2021).

[25] FORTA Concrete Fiber, “Forta Ferro,” 2021. http://www.forta-ferro.com/products/forta-ferro/ (accessed Jul. 01, 2021).

[26] Durable Products Group LLC, “SafeTcrete PRECAST Maximum Performance Fiber.” https://www.duratechnologies.com/safetcrete-precast/ (accessed Jul. 01, 2021).

[27] Euclid Chemical, “Euclid Chemical Fiber Datasheet”, www.euclidchemical.com

[28] Arkansas State Highway and Transportation Department, “2014 Standard Specifications for Highway Construction,” 2014.

[29] ASTM Standard C192/C192M, 2020, “Standard Practice for Making and Curing Concrete Test Specimens in the Laboratory”, ASTM International, West Conshohocken, PA, 2020, DOI: 10.1520/C0192_C0192M-19, www.astm.org.

[30] ASTM Standard C494/C494M, 2021, “Standard Specification for Chemical Admixtures for Concrete”, ASTM International, West Conshohocken, PA, DOI: 10.1520/C0494_C0494M-19, www.astm.org.

[31] U.S. Department of Transportation - Federal Highway Administration, “Texture of Concrete Pavements - Observations from the FHWA Mobile Concrete Trailer (MCT)”.

[32] C. Zanotti and N. Banthia, “Modified Slant Shear Cylinder Test for Inherent Characterization of Bond in Concrete Repairs”, *The Indian Concrete Journal*, vol. 90, 2016.

[33] ASTM Standard C39/C39M, 2021, “Standard Test Method for Compressive Strength of Cylindrical Concrete Specimens”, ASTM International, West Conshohocken, PA, 2021, DOI: 10.1520/C0039_C0039M-21, www.astm.org.

[34] ASTM Standard C882/C882M, 2021, “Standard Test Method for Bond Strength of Epoxy-Resin Systems Used With Concrete By Slant Shear”, ASTM International, West Conshohocken, PA, 2021, DOI: 10.1520/C0882_C0882M-20, www.astm.org.

[35] ASTM Standard C1609/C1609M, 2020, “Standard Test Method for Flexural Performance of Fiber-Reinforced Concrete (Using Beam With Third-Point Loading)”, ASTM International, West Conshohocken, PA, 2020, DOI: 10.1520/C1609_C1609M-19A, www.astm.org.

[36] A. P. Fantilli, H. Mihashi, and P. Vallini, “Multiple Cracking and Strain Hardening in Fiber-Reinforced Concrete Under Uniaxial Tension”, *Cement and Concrete Research*, 2009, DOI: 10.1016/j.cemconres.2009.08.020.

[37] American Concrete Institute Committee 318, *Building Code Requirements for Structural Concrete (ACI 318-14) and Commentary (ACI 318R-14)*. American Concrete Institute, 2014.

[38] ASTM Standard C1018, 2021, “Standard Test Method for Flexural Toughness and First-Crack Strength of Fiber-Reinforced Concrete (Using Beam With Third-Point Loading)”, ASTM International, West Conshohocken, PA, 2021, www.astm.org.